Hydrological Processes

WILEY

RESEARCH ARTICLE OPEN ACCESS

Flood Risk Management Using Representative Hillslopes: Insights From a Historical Flood in Southwest Germany

Ashish Manoj J. | Franziska Villinger | Jan Wienhöfer | Ralf Loritz | Erwin Zehe

Chair of Hydrology, Institute of Water and Environment (IWU), Karlsruhe Institute of Technology, Karlsruhe, Germany

Correspondence: Ashish Manoj J. (ashish.jaseetha@kit.edu)

Received: 9 January 2026 | **Revised:** 14 April 2026 | **Accepted:** 16 April 2026

Keywords: convective storms | flash flood | Hortonian overland flow | landuse | mitigation | nature-based solutions | reconstruction | representative hillslopes

ABSTRACT

Understanding and preparing for extreme events in a warming climate remains challenging, particularly for modelling flash floods in small- to mesoscale catchments. While top-down modelling approaches that describe fluxes at the system scale are often effective for riverine floods driven by saturation-excess runoff, bottom-up approaches are better suited to capturing intensity-controlled runoff generation and associated preferential flow processes. Based on the gradient-conserving simplification of representative hillslopes, a meso-catchment scale spatially distributed, process-based model was applied to simulate a severe summer flood event that occurred in 1994 in southwest Germany. Our approach provides a balance between the complexity required to represent coupled flow processes at the hillslope scale and the practical constraints of scaling these to the mesoscale. Following evaluation against available observations, the model is used to reconstruct flood magnitudes in poorly gauged but severely affected headwater regions in the catchment. The results highlight the influence of spatial variability in gradients and land use on runoff generation in these areas. To further explore these findings, we conducted additional simulations across a range of precipitation return periods to examine the sensitivity of flood response under different scenarios. The results suggest that uncertainties are more pronounced at smaller spatial scales, likely due to data limitations. Finally, simplified nature-based solution (NbS) scenarios were implemented at the hillslope and headwater scales to explore their potential influence on downstream flood response. This study contributes to improved understanding of overland flow responses over mesoscale catchments, a critical scale for flood management, particularly under increasing convective extremes as a result of anthropogenic climate change.

1 | Introduction

Floods are usually defined as the inundation of an otherwise dry area or a significant streamflow event extending well beyond the regular river banks (Mishra et al. 2022). They can result from various atmospheric processes (Merz et al. 2021), which are then modulated by local catchment and river network dynamics, and are heavily impacted by anthropogenic climate change (Pall et al. 2007) and other human induced modifications. Flood risk management can be improved by adopting better modelling strategies (Brunner et al. 2021) that explicitly account for the rarity of such events.

Unlike floods controlled by storage (saturation excess—Dunne 1978) or driven by channel networks (Merz et al. 2021), flash floods typically result from Hortonian overland flow (Horton 1933), which is usually driven by convective storm activity (Meyer et al. 2022) in small headwater catchments and influenced by localised preferential flow processes, such as macropore flow.

It is important to emphasise that the flow patterns and subsequent attenuation of flood waves in river channels (Fenton 2019) are more thoroughly observed and characterised than the localised processes (Bronstert et al. 2023)

occurring at the hillslope scale. These localised processes may include, but are not limited to, antecedent conditions, re-infiltration, surface sealing, and the activation of preferential macropore flow. These nonlinear processes interact to create significant and evolving hazards, whose impacts cannot be accurately predicted by generalised linear models (Kirkby and Cerdà 2021; Nash 1957).

Conversely, as shown by recent advances in so-called nature-based solutions (NbSs-(Guillaume et al. 2025; Richet et al. 2017; Rosier et al. 2024)), localised, site-specific water retention measures could attenuate the flood at the cause scale (e.g., hedgerows at agricultural fields) rather than seeking measures to tackle the flood at the effect scale (e.g., flood reservoirs near the catchment outlet).

Spatially distributed, process-based modelling approaches (Fatichi et al. 2016) have much to offer to tackle the challenges associated with such intensity-controlled events. These models rely on correctly representing the gradients driving the flow, hence requiring far fewer events for model learning. Transfer learning implies that parameter values from catchments sharing similar characteristics could be used throughout the entire region. They also enable the virtual implementation of NbS at the hillslope scale, allowing for intricate details such as the spatial arrangement of these measures with respect to the dominant flow paths within the catchment.

One potential drawback of using such models is their high demand for data and computational complexity. This consideration becomes increasingly important in design, where rapid and cost-effective alternatives are usually preferred. Innovative catchment simplifications that maintain the system's total flow potential could effectively balance computational complexity with necessary process representation. One such approximation is the concept of *representative hillslopes* (Loritz et al. 2017) which tries to model only a fictitious representative hillslope profile derived from the topology of all existing hillslopes within a catchment. While the concept has shown promising results in smaller experimental catchments (Loritz et al. 2017; Villinger et al. 2022) and recently to predict flash floods in poorly gauged headwater catchments (Manoj et al. 2024). It remains to be seen how such simplifications impact process representation and model performance at the larger mesoscale.

Flood risk management should ideally also take care of 'surprises' (Mishra et al. 2022). A growing concern is the failure of flood retention structures designed for a T-year return period when faced with a storm that has a return period shorter than T. Idealised design workflows often overlook responses to short-duration events that mainly trigger intensity-controlled (Hortonian) runoff generation. This issue is exacerbated in some cases due to the lack of records for past destructive flooding episodes, especially those that occurred in localised (often poorly gauged) headwater catchments.

At the hillslope scale, non-linearities and complexities due to changing landuse patterns significantly influence the shape of the flood hydrograph. However, flood management practices often focus on much larger scales, typically due to social and administrative constraints. Changes in land use, especially soil sealing, compaction, and the removal of hedgerows, have contributed to increased water loss through runoff in post-World War II Europe (Auerswald et al. 2025). On the other hand, if implemented properly, such changes have the potential to mitigate some of the adverse effects of global warming on terrestrial environments. Unfortunately, they are neither adequately represented in hydrological models nor considered a viable pathway to achieving sustainability goals.

With the following challenges in mind, in this study, we explore:

a. How does upscaling representative hillslopes, derived from the average topographic gradient at the subbasin scale, to the mesoscale through hydraulic routing influence the simulation of runoff generation processes and flood dynamics during convective events?

b. What do reconstructed flood events reveal about the dominant runoff generation mechanisms, including the role of preferential flow, and the validity of existing flood design assumptions in the catchment?

c. Is it possible to provide protection against such flash floods at the larger meso-scale by using localised NbS on the hillslope scale?

2 | Venue and Modelling Philosophy

2.1 | Study Area

The Elsenz Schwarzbach catchment (located in the federal state of Baden-Württemberg, Germany) was chosen as the study area (Figure 1), as it was severely impacted during the catastrophic 1993–1994 (Disse and Engel 2001; Villinger et al. 2022) flood series in Germany. The German federal state of Baden-Württemberg lies toward the country's southwest, sharing land borders with France and Switzerland. The two major climatic regimes according to the Köppen-Geiger classification (Beck et al. 2018) are temperate oceanic climate (Cfb) and humid and warm continental climate (Dfb). The state is primarily drained by the subcatchments of the Rhine, with the rest by the Danube catchments (Ho et al. 2025).

This medium sized mesoscale catchment (196 km^2; Figure 1), while being largely hydrologically unobserved (except for streamflow) shares similar geological and pedological characteristic as the heavily experimented (but smaller: 3.5 km^2) Weiherbach catchment (Figure A1 in Appendix A) (Zehe et al. 2001). Both the catchments lie in the 'Kraichgau' region, mainly consisting of agricultural catchments with Loess soils. The Elsenz Schwarzbach drains into the Neckar river at Neckargemünd. The river Neckar then joins the Rhine river at Mannheim.

During the convective storm-driven summer flood (27 June) of 1994 (Appendix B), an estimated destruction (Figure B2 in Appendix B) of 250–300 million Deutsche Mark was reported (Henkel 1994) in the 10 municipalities within the Elsenz Schwarzbach catchment (Appendix B). Sadly, three human fatalities were also reported for the event. The most severely affected (Vogt 2024) where the towns of Eschelbronn, Helmstadt,

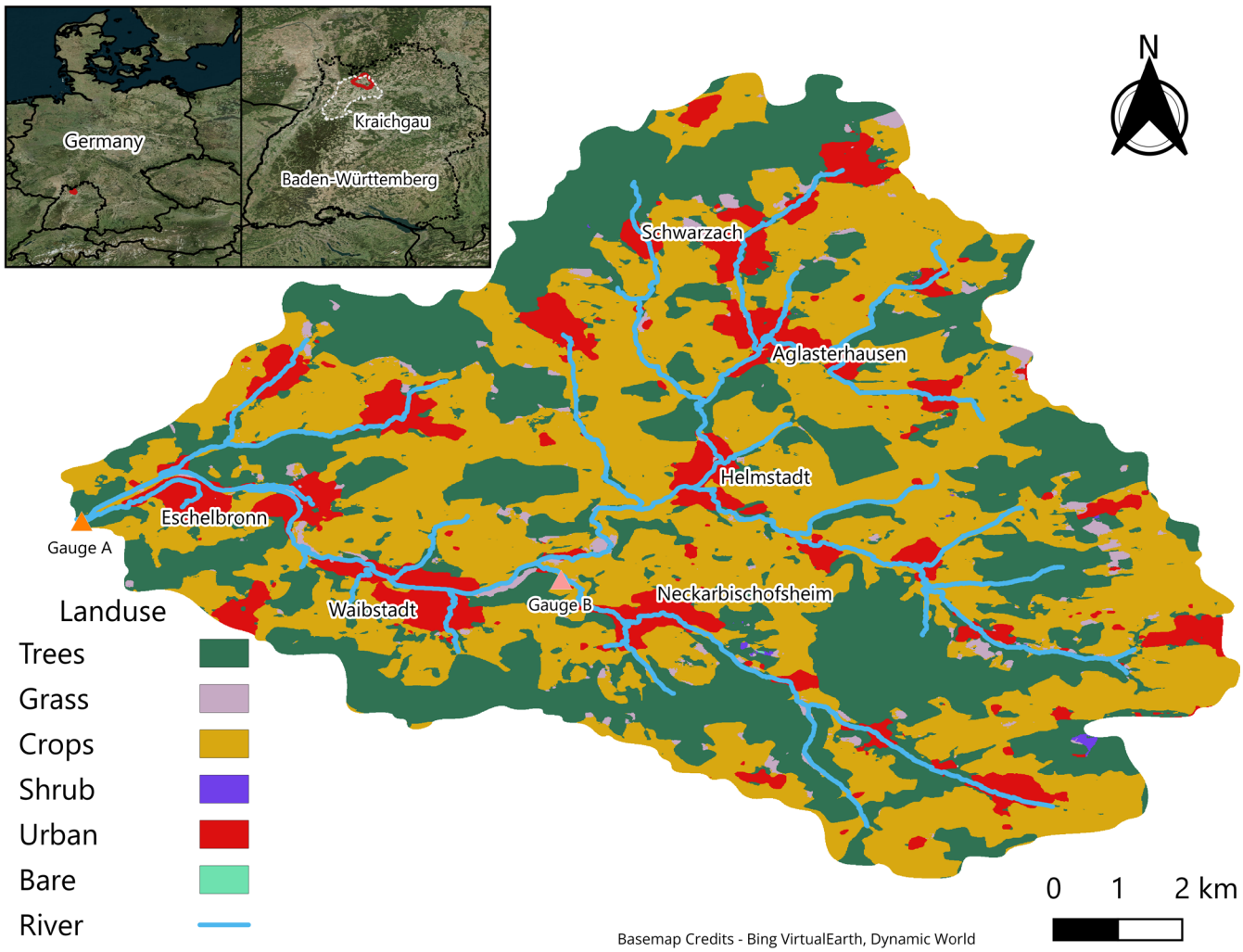

FIGURE 1 | Land cover map of the predominantly agricultural and forested Elsenz–Schwarzbach catchment, showing the locations of major population centres (see also Figure A4 in Appendix A). The inset indicates the catchment's location within Baden-Württemberg, Germany.

Waibstadt, and Neckarbischofsheim (Figures 1 and A6 in Appendix A). The temporal preconditioning of the event by the winter floods of 1993–1994 also led to a compounding of impacts (Ruiter et al. 2020) in the region. Due to these catastrophic flooding episodes in 1993–1994, a comprehensive flood protection concept (Zweckverband Hochwasserschutz Elsenz-Schwarzbach 2016) was developed for the entire region, leading to the construction of local flood retention basins throughout the catchment area. Around 20 flood reservoirs are now operational within the catchment with a combined design flood storage volume of 885 000 m^3. The region again faced a severe convective storm clustering in June 2016, leading to localised flash floods (Manoj et al. 2024) overtopping the flood reservoirs in some regions (Figure B4 in Appendix B).

2.2 | Representative Hillslopes

Balancing the intricacies required for process based models with the required simplicity stemming from parsimony considerations (Hrachowitz and Clark 2017) has long been considered one of the holy grails of hydrology. While top-down approaches (such as the unit hydrograph) offer readily applicable solutions, they are often criticised for their simplifying assumptions. Models resting on bottom-up paradigms (Fatichi et al. 2016), on the other hand, demand a larger parameter space and higher computational complexity.

The concept of representative hillslopes (Loritz et al. 2017) is an attempt to bridge the gap between these two worlds. Building upon related works (Cochrane and Flanagan 2003; Francke et al. 2008) on deriving representative hillslope catena for catchments, the approach addresses the question of what is a meaningful approximation for the large number of dominant flow paths in a hydrological system, and up to what scale do such approximations hold good. By creating and modelling a *fictitious* hillslope (which doesn't really exist in the system but is rather an derivation of the averaged distribution of potential energy of all the existing hillslopes along the averaged distance to river), the approach shows commendable results (Loritz et al. 2017; Manoj et al. 2024; Villinger et al. 2022) in reproducing the rainfall-runoff behaviour in headwater catchments up to 20 km^2. Here we expand this concept to the scale of the entire Elsenz Schwarzbach catchment—the idea is to connect representative hillslope models for the sub-catchments with river network and a hydraulic routing scheme.

2.3 | Modelling Approach

2.3.1 | Hydrological Model

Beginning from around 1990, the Weiherbach catchment (Figure A1 in Appendix A) in the Kraichgau region was the focus of detailed experiments on the interplay between infiltration, runoff generation and related transport processes of solutes and sediments with a focus on explanatory, physically based modelling (Bronstert et al. 2023; Zehe et al. 2001). The spatially distributed, process based hydrological model CATFLOW (Zehe et al. 2001) was developed as part of this detailed field investigations. The basic modelling unit is a 2D hillslope. Water and solute dynamics of each hillslope element are simulated on a terrain following curvilinear grid. Therefore, the fundamental equations for mass and water transport must be transformed from their typical Cartesian form into curvilinear coordinates.

Assuming that $u(\eta,\xi)$ and $v(\eta,\xi)$ are the mapping functions of the curvilinear coordinate directions η and ξ into the cartesian coordinates x and z such that.

$$\begin{aligned} x &= u(\eta,\xi) \\ z &= v(\eta,\xi) \end{aligned} \tag{2.1}$$

Since the physical line element (distance, $ds^2 = dx^2 + dy^2 = d\eta^2 + d\xi^2$) has to be invariant under the transformation and by using chain rule of differentiation successively:

$$\begin{aligned} \frac{\partial}{\partial x} &= \frac{1}{f^{\xi}}\frac{\partial}{\partial \xi} \\ \frac{\partial}{\partial y} &= \frac{1}{f^{\eta}}\frac{\partial}{\partial \eta} \end{aligned} \tag{2.2}$$

where are the metric coefficients that have to be evaluated locally at each grid point. The use of curvilinear coordinates simplifies modelling complex hillslope soil surfaces, allowing for more accurate representation of surface runoff and erosion processes.

$$\begin{aligned} f^{\xi} &= \left(\frac{\partial u}{\partial \xi}\right)^2 + \left(\frac{\partial v}{\partial \xi}\right)^2 \\ f^{\eta} &= \left(\frac{\partial u}{\partial \eta}\right)^2 + \left(\frac{\partial v}{\partial \eta}\right)^2 \end{aligned} \tag{2.3}$$

Soil water dynamics within the hillslopes are then characterised using the 2D Darcy–Richards equation in these transformed curvilinear coordinates.

$$\begin{aligned} \frac{\partial \theta}{\partial t} = \frac{1}{f^{\xi}}\frac{\partial}{\partial \xi}\left\{K(\theta)\left[k^{\xi\xi}\frac{1}{f^{\xi}}\frac{\partial}{\partial \xi}(z-\psi) + k^{\xi\eta}\frac{1}{f^{\eta}}\frac{\partial}{\partial \eta}(z-\psi)\right]\right\} + \\ \frac{1}{f^{\eta}}\frac{\partial}{\partial \eta}\left\{K(\theta)\left[k^{\eta\xi}\frac{1}{f^{\xi}}\frac{\partial}{\partial \xi}(z-\psi) + k^{\eta\eta}\frac{1}{f^{\eta}}\frac{\partial}{\partial \eta}(z-\psi)\right]\right\} - \omega \end{aligned} \tag{2.4}$$

The coefficients $k^{\xi\xi}, k^{\eta\eta}, k^{\xi\eta}$ account for the anisotropy of the hydraulic conductivity and ω represents the source and sink terms. The soil hydraulic conductivity $K(\theta)$ as a function of the relative saturation, S and the soil water retention function (the soil water content, θ as a function of the matrix potential (ψ) can be parameterized according to van Genuchten (1980) and Mualem (1976), Tang and Skaggs (1977) or the recently proposed PDI model (Peters et al. 2021).

Overland flow heights are simulated using the diffusion wave approximation to the Saint-Venant equation and explicit upstreaming, in combination with the Gauckler-Manning-Strickler formula (Hager 2015).

The model can represent preferential macropore flow by using an effective macroporosity factor. This factor (Loritz et al. 2017; Wienhofer and Zehe 2014) scales the ratio of infiltration into the macropore domain compared to the matrix domain.

For the effective macroporosity factor approach, as detailed in Zehe et al. (2001), the bulk hydraulic conductivity k_s^B, is linearly increased by a relative scaling factor, f_m (if relative saturation (S) at a grid point exceeds a certain specified threshold (S_o) but only till complete saturation) as follows:

$$\begin{aligned} k_s^B &= k_s + k_s f_m \frac{S - S_o}{1 - S_o} \ \text{if}\ S_o \le S < 1 \\ k_s^B &= k_s \ \text{otherwise} \end{aligned} \tag{2.5}$$

Thus, emulating the preferential flow paths (of increased saturated hydraulic conductivity and consequently larger flow velocities) through which water could flow to the deeper layers in the hillslope.

2.3.2 | River Routing Model

The river routing model, which connects the subbasins through the main channel, uses a one-dimensional kinematic wave approximation of the Saint-Venant equations (Fenton 2019; Troy et al. 2025). The law of conservation of mass is expressed as follows:

$$\frac{\partial Q}{\partial x} + \frac{\partial A}{\partial t} = q \tag{2.6}$$

where Q is streamflow, x is distance along the river channel, A is the cross-sectional area of the river channel, t is time, and q is the lateral flow from the representative hillslopes into the river channel. Under the kinematic wave approximation, local and convective acceleration as well as pressure gradient terms, are neglected in the full dynamic momentum equation, and the friction slope (s_o) is assumed equal to the bed slope (s_f). The momentum equation then reduces to an algebraic relation between streamflow, Q and the flow area, A. The Gauckler-Manning-Strickler formula is then used for the same.

$$Q = K_{st}\sqrt{s_o}\,(A/P)^{\frac{2}{3}}\,A \tag{2.7}$$

where P is the wetted perimeter, A is the wetted cross section, and K_{st} is the strickler roughness coefficient (which is also more commonly expressed as inverse of the Manning roughness coefficient, n). Equation (2.7) is then substituted into Equation (2.6), resulting in one equation with one

unknown. This is then solved using a finite difference scheme that enforces a Courant condition on the time step, ensuring numerical stability and monotonicity of the solution, thereby suppressing numerical dispersion.

3 | Methodology

3.1 | Setting Up the Model

3.1.1 | System Geometry

The representative hillslope profile lines were extracted individually for all the subbasins (124 in total: Figure 2A) of the Elsenz Schwarzbach in parallel using the workflow outlined in Appendix C. Figure 2 depicts the main methodological steps involved in the extraction process of one such representative hillslope profile (Figure 2B). Firstly, the digital elevation model is preprocessed to fill all depressions and sinks. This is followed by the extraction of other rasters (Figure 2C). It is important to highlight that the DEM source, its spatial resolution (10 m), and the GIS-based processing routines may introduce uncertainties (Table 1) in the derivation of hillslope profiles. These uncertainties can influence the representation of terrain morphology, including slope gradients and flow pathways.

The relative elevation of each cell above the nearest stream segment and the corresponding distance to the stream segment define the flow profile lines (Figure 2B) in each subbasin. Flow profile lines can be defined as the paths water takes as it flows from one cell to the next, starting from a cell with no water inflow at the hillcrest and terminating at a river cell. Our aim is to derive a single representative hillslope for the subbasin rather than modeling all these flow profile lines individually. This is done by considering the total potential energy of all the hillslopes (Manoj et al. 2024).

Preserving this total energy implies that topography of the new representative hillslope should be chosen to maintain average topographic gradients along the flow path. We achieve this by binning the geopotential energy based on proximity to the river and then performing a weighted average (Francke et al. 2008) using the flow accumulation values within each segment. Consider all the cells (Figure 2B) at a relative distance of x m from the nearest stream cell, we require an estimate of relative elevation, $\bar{h}(x)$ for our representative hillslope, by evaluating the elevation (h) of all cells, at the same distance. This elevation is obtained by multiplying the elevation of each cell by their corresponding flow accumulation values (f), which denotes the number of flow profile lines that pass through a cell and hence its relative importance. The process is then repeated for all the binning distances.

$$\bar{h}(x) = \frac{\sum_{i=1}^{\text{All cells at } x} h_i^x \sqrt{f_i^x}}{\sum_{i=1}^{\text{All cells at } x} \sqrt{f_i^x}} \tag{3.1}$$

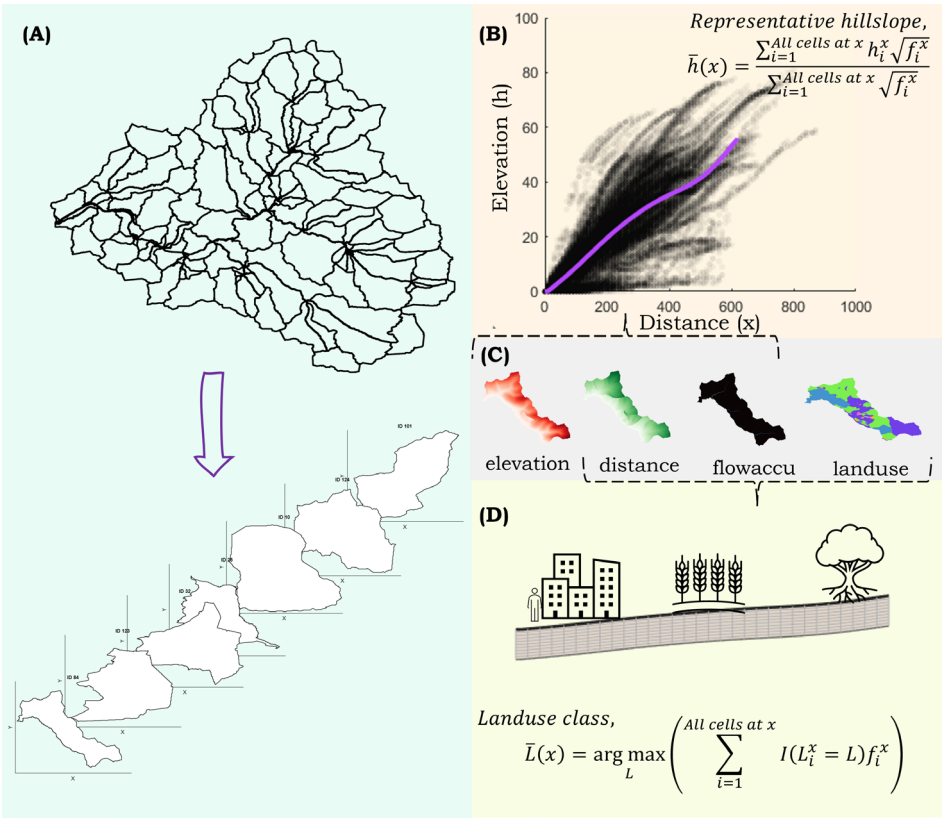

FIGURE 2 | Schematic overview of the representative hillslope derivation. The catchment is first divided into different subbasins (A), the representative hillslope profile for each subbasin (B) is derived from the elevation, distance and flow accumulation raster files (C). A similar approach is utilised to get the landuse distribution along each representative hillslope (D). The process is then repeated for all the subbasins in the catchment (A) in parallel using the reproducible research workflow detailed in Appendix C.

TABLE 1 | Methodological overview of the different parameters used for setting up the model.

Type of information	Parameter/Property	Estimation method (Transfer/Calibration)	Sources of uncertainty/ Alternative values	References
System Geometry	Representative hillslopes	Derived directly from topographic information	Uncertainties arising from DEM data quality, resolution limitations, and GIS-based terrain processing steps	Loritz et al. (2017) & Zehe et al. (2014)
	Manning strickler values for channel network (K_{st})	Assigned based on increasing Strahler order and literature values	Variations in channel roughness do not affect the overall conservation of total storm runoff volume	Strahler (1957) and Te Chow (1959)
System Parameterisation	Soil hydraulic properties	Transferred directly from literature values obtained from undisturbed soil samples in the Weiherbach	Could also be derived using soil pedotransfer functions from openly available textural data	Table 3 in Zehe et al. (2001)
	Relative hillslope catena	Transferred from previous experiments	Set up was also used to derive flash flood estimates for a 2016 storm in Elsenz Schwarzbach	Zehe et al. (2001) and Manoj et al. (2024)
	Manning strickler values for landuse classes (K_{st})	Transferred directly from literature values obtained from sprinkling experiments in the Weiherbach	Relative position of classes derived to maintain the landuse gradient	Tab 5 in Zehe et al. (2001)
	Macroporosity scaling factor (f_m)	Transferred directly from literature values	Previous studies report a scaling in the range of one order of magnitude	Niehoff et al. (2002) and Bronstert et al. (2023)
	Extent of macropore flow (l)	Transferred from previous experiments in the same catchment	Set up used to derive flash flood estimates for a 2016 storm in Elsenz Schwarzbach	Manoj et al. (2024)
System Initialisation	Antecedent conditions	Initialised using ERA5 Land soil moisture bands	Initialisation using ERA5 Land showed commendable goodness of fit in an earlier study over the same region	Muñoz-Sabater et al. (2021) and Manoj et al. (2024)
	Daily accumulated precipitation sums	Obtained from the HYRAS gridded product	Interpolation uncertainty	Rauthe et al. (2013)
	Precipitation intensity timeseries	Transferred from previous experiments in the Weiherbach	Observational uncertainty	Villinger et al. (2022)

Interested readers are referred to Loritz et al. (2017) and Manoj et al. (2024) for a validation of the total energy conservation using different distance classes and a more detailed explanation of the methodology. The same process is then repeated for all the other subbasins (Figures A2 and C1).

We converted the stream network (Figure A3) of the entire catchment into a system of interconnected channel nodes, connecting each representative hillslope at the location of the corresponding sub-basin outlet. The 1D kinematic wave routing was established to model the propagation of the flood wave along the channel network. Due to the absence of detailed field data, the Gauckler-Manning-Strickler roughness (Throughout the remainder of this work, we use both Manning's roughness and Strickler values interchangeably to refer to the roughness coefficient (K_{st}) in the Gauckler-Manning-Strickler formula. Interested readers are referred to Hager 2015 for a historical anecdote) coefficients for stream routing (Table 1) were assigned based on literature values (United States Geological Survey 1989; Te Chow 1959).

Lower-order streams tend to be narrower, more vegetated, or irregular, resulting in greater resistance to flow than the well-defined, larger, higher-order channels (Heldmyer et al. 2022). Consequently, streams with a higher Strahler stream order (Strahler 1957) were assigned correspondingly higher Strickler values, as indicated in Table 2.

3.1.2 | Soil and Landuse Mapping

The mesoscale catchment shares similar geological and pedological characteristics with the heavily experimented Weiherbach catchment (Zehe et al. 2001). Hence, we transferred the relative hillslope soil distribution profile (Loess and Coluvisols) and corresponding hydraulic functions (which include the van Genuchten parameters: See tab. 4 in Zehe et al. 2001) for these soils from the Weiherbach catchment.

Accurate land-use scenarios are a prerequisite for assessing the impact of landuse gradients on runoff generation at the catchment scale. We use the Dynamic World landuse dataset (Brown et al. 2022) for mapping the dominant landuse classes in our catchment. The classification taxonomy involves nine dominant classes. The relevant classes in our study area (Figures 1 and A4) and the corresponding Manning roughness values chosen (again informed from the Weiherbach field experiments: Zehe et al. 2001) are shown in Table 3.

TABLE 2 | Gauckler-Manning-Strickler coefficient values for different stream orders.

Stream order	Gauckler-Manning-Strickler coefficient (K_{st}-$m^{1/3}s^{-1}$)
1	15
2	20
3	30
4	40

For each subbasin (and corresponding representative hillslope), we now require the relative distribution of the different landuse classes along the gradient. This is done analogously to our extraction of the representative hillslope profiles. We were interested in getting a mean value for elevation there; here, the focus shifts to getting the dominant landuse class for each distance (Figure 2D). This is attempted by looking at the relative flow accumulation values for each cell with a specified landuse class. Instead of a weighted average, we choose the class with the largest areal share.

To determine the representative land-use class $\overline{L}(x)$ at a relative distance of xm from the nearest stream cell, we consider all raster cells located at that same distance in the different hillslope profiles (Figure 2B). For this group of cells, we evaluate the land-use category by weighting each class (L) according to the flow accumulation of the cells that belong to it. Thus, giving greater influence to cells through which many flow profiles pass. We then sum the weighted contributions for each landuse class separately. Finally, choosing the class with the highest value for this weighted sum as the representative landuse class element at this distance. Mathematically (Equation 3.2), we seek a value L that maximises the weighted sum of the indicator function $I(L_i = L)$, which equals 1 when a cell belongs to the class L and 0 otherwise; multiplied by its corresponding flow-accumulation value f_i.

$$\overline{L}(x) = \arg\max_{L} \left(\sum_{i=1}^{\text{All cells at } x} I\left(L_i^x = L\right) f_i^x \right) \tag{3.2}$$

3.1.3 | Initial and Boundary Conditions

Previous works (Liu et al. 2025) have demonstrated that initialising a process-based model with climate reanalysis data can help address the challenges of data availability in data-scarce regions. In a previous study conducted in headwater catchments within the same region (Manoj et al. 2024), ERA5-Land (Muñoz-Sabater et al. 2021) soil moisture bands was used for model initialisation, and the resulting CATFLOW simulations were compared with multiple soil moisture products (ERA5-Land, GLEAM, GLDAS, and MERRA). While CATFLOW simulations were consistently drier than ERA5-Land, strong correlations were observed across all datasets, indicating consistency in temporal dynamics.

TABLE 3 | Gauckler-Manning-Strickler Coefficient values for different landuse classes.

Landuse ID	Class	Gauckler-Manning-Strickler coefficient (K_{st}-$m^{1/3}s^{-1}$)
1	Trees	8
2	Grass	10
4	Crops	9
5	Shrub	10
6	Urban	30
7	Bare earth	12

While we do not expect a direct match between CATFLOW and large-scale land surface model products due to differences in spatial resolution, vertical discretisation, and hydraulic parameterisation. However, for initialisation purposes, capturing relative saturation values is more critical than matching absolute values.

For our simulation of the historical flood that occurred in June 1994, we again opted to use ERA5 Land Reanalysis to initialise the model. The initial conditions for each model run were derived (after normalisation) from the hourly soil moisture band values, specifically: "volumetric_soil_water_layer_1-4", from the ERA5 Land reanalysis product. The absolute soil moisture values from the land surface model were converted to relative saturation values using porosity and residual soil moisture parameters, and these relative saturation values were then used to initialise the hillslope models. A sensitivity analysis was then conducted to look at the benefit of such an initialisation compared to a random guess of the soil moisture states.

For the historical summer flood of 1994 (Appendix B), gauges with finer resolution precipitation estimates are unfortunately not available within the catchment boundary of the Elsenz Schwarzbach, while the German Weather Services provides daily accumulated sums (DWD 2024; Rauthe et al. 2013) in the HYRAS gridded product (our study area received an average precipitation of 90 mm: Figure B1) this is not enough for estimating the dynamics of flash flood generation due to intensity excess Hortonian flow. To overcome this limitation of forcing data, we make use of the quality checked higher resolution (6 min) precipitation data (Figure 3) recorded at the gauging station (Zehe et al. 2001) in Weiherbach experimental catchment (total sum—83 mm). Since the Weiherbach catchment also had a strong runoff reaction (Villinger et al. 2022) during the event and due to its spatial proximity (around 20 km), we assume that the storm intensity distribution is similar. We derive daily sums individually for each subbasin (representative hillslope) in our catchment and then assume the same distribution (rainfall hyetograph) of storm as recorded in the Weiherbach gauge. The derived series is then used to simulate each representative hillslope separately. To examine the sensitivity and applicability of the transfer, we performed additional simulations with alternative rainfall intensity distributions, including one derived from radar observations in the Elsenz Schwarzbach catchment during the summer flash flood of 2016 (Manoj et al. 2024) and another based on a synthetic triangular distribution with an assumed storm duration of 2 h (Figure 3). In addition, to further test the validity of our model setup, we simulated a more recent flood event from April 2023 using high resolution radar based precipitation estimates of the actual event from the German Weather Service (DWD 2021).

3.2 | Simulating Design Adequacy

In Germany, flood reservoirs are typically designed in accordance with the DIN 19700 standard (LUBW 2007). Dams are classified into four categories based on their height and capacity: very small, small, medium, and large reservoirs. The design must account for a flood event with a return period of 50–10 000 years, depending on the category of the reservoir. The German Weather Services and the State Institute of Environment, Baden-Württemberg (LUBW) provide location specific standardised estimates for extreme precipitation sums corresponding to different return periods and storm durations (DWD 2023; Junghänel et al. 2017; LUBW 2023) which are then used for design purposes. We applied the validated model to five scenario-based simulations to explore flood responses across a range of return periods (Table 4) along the Elsenz–Schwarzbach, assuming a storm duration comparable to the 1994 event.

3.3 | Exploring Nature Based Solutions (NbS)

Historically, vegetative features such as hedgerows were integral to agricultural landscapes, marking the boundaries of

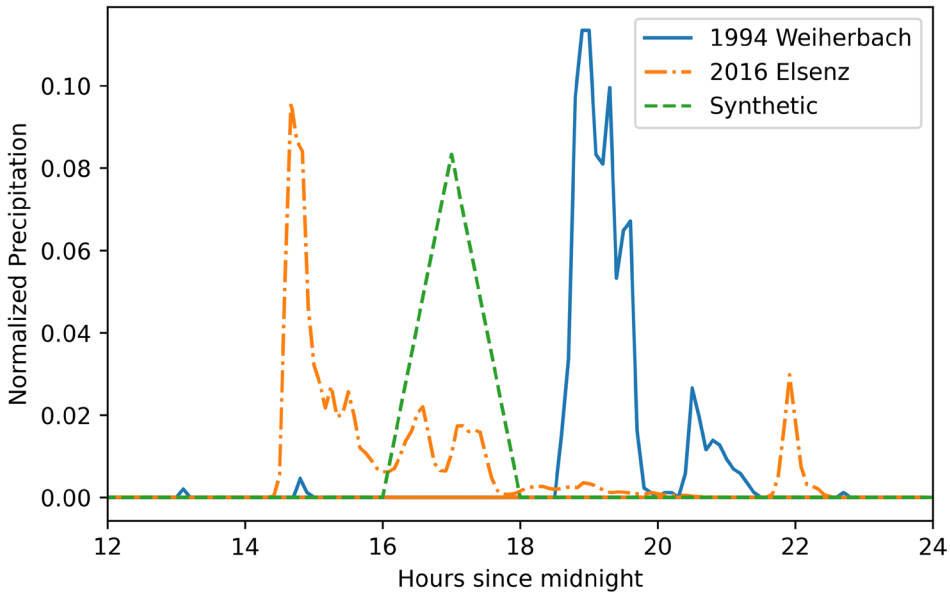

FIGURE 3 | Normalised precipitation intensity timeseries considered in the study.

TABLE 4 | Design precipitation sums for different return period floods according to DWD (2023) and LUBW (2023).

Return period (years)	Precipitation (mm)
100	55.73
200	61.5
500	69
1000	74.5
10000	93

individual landowners' plots. This network of vegetation provided significant benefits to the catchment's surface hydrology (Rosier et al. 2024). By creating impediments to overland flow, hedgerows slowed down water movement and enhanced soil infiltration. However, due to a lack of previous scientific evidence (Rosier et al. 2023) supporting their effectiveness and to changes in land ownership patterns (most notably the shift from smaller to larger consolidated fields), these elements have largely disappeared from many agricultural regions in Europe. After the 1994 floods in the Elsenz Schwarzbach, the consequences of disappearing hedgerows (Figure B3 in Appendix B) once again became a topic of discussion, as evidenced by historical newspaper archives (Henkel 1994) from that period. On the other hand, contemporary forest management practices often involve the use of heavy machinery, which has seen an increase in wheel loads (Auerswald et al. 2025) over the past century. This has resulted in increased subsoil compaction (Brus and van den Akker 2018; Schneider and Don 2019), further diminishing the infiltration capacity of the soil.

To explore the potential influence of NbS on the 1994 flood response, we implemented a set of simplified, scenario-based modifications for different land use classes (Figure 2D and Table 3) within the catchment. The first scenario represents the introduction of hedgerow elements (Rosier et al. 2024, 2023) within agricultural areas (landuse class—crops; Table 3). The second scenario considers reduced soil compaction in forested areas (landuse class—trees; Table 3), such as through the use of designated skid trails for heavy machinery (Auerswald et al. 2025).

For the hedgerow scenario, continuous stretches of cropland within the representative hillslope were identified, and a hedgerow element was placed approximately at the midpoint of each stretch, with a length corresponding to about 10% of the cropped area. The reduced-compaction scenario was applied uniformly across forested portions of the representative hillslopes.

While substantial research has been conducted to understand how these NbS influence key parameters in hydrological modelling, uncertainties persist, as their effects are highly location-specific. In this study, we utilise recommendations based on previous research (Guillaume et al. 2025; Richet et al. 2017) about the Manning-Strickler roughness (K_{st}), saturated hydraulic conductivity (k_{sat}) and saturated water content of soils (Θ_{sat}). This focus is primarily due to the study regions located in France (Richet et al. 2017) and Belgium (Guillaume et al. 2025), included agricultural loess soils similar to the Elsenz Schwarzbach in Germany. The parameter values for the new hedgerow landuse class were provided and modified for the tree landuse class as outlined in Table 5. These schematic implementations are intended to provide an exploratory hydrologic assessment of how such measures may influence runoff generation and flood response, rather than a site-specific or quantitatively validated evaluation of NbS performance in our region.

4 | Results

4.1 | Model Building and Testing

We simulated representative hillslopes using the CATFLOW hydrological model for all subbasins of the Elsenz Schwarzbach during the 1994 summer event and then used the 1D channel routing to estimate the flood at the outlet (Gauge A).

Figure 4 shows the overestimation of the observed flood dynamics by our initial modelled set-up. These overestimations align with findings from other studies (Beven and Germann 1982; Bronstert et al. 2023; Niehoff et al. 2002; Weiler 2006), which reports that in soils with very low soil hydraulic conductivity (as in our case with the agricultural loess soils), when confronted with high intensity rainfall during convective storms, a large part of infiltration may pass through so-called soil macropores into deeper soil layers, thus not contributing to overland runoff.

To simulate the effect of macropore flow (Table 1) during the high intensity storm of 1994, we used the simplified macroporosity approach (Equation 2.5). This essentially replicates the increased infiltration due to macropore flow by relative scaling of the bulk hydraulic conductivity along the representative hillslope element. A scaling factor of 10 is chosen, consistent with findings from other studies in the regions (Manoj et al. 2024; Niehoff et al. 2002). We assume increased macropore flow along 90% of the hillslope catena. The hillslopes are again simulated, considering the macropore effect. As expected, the new flood simulated flood hydrograph with macropores is closer to the observed curve (with a Nash Sutcliffe Efficiency (Nash and Sutcliffe 1970) value of 0.58). The total flood volume (Table 6) aligns closely with the observed flood volume (relative error of −12%). We also observed that the dynamics of the flood are well captured. The model accurately captures the rise of the flood wave at around 20:00 CET and 04:00 (+1 day) CET. While there are some overestimations and sharper recessions (possibly due to our choice of 1D hydraulic routing), the model captures the flood peak with a relative error of −24%. The subsequent return to normal flow levels is the same in both runs at around 12:00 CET (+1 day). It is interesting to see that the flood response still clearly reflects the temporal pattern of the rainfall event, even though the latter is an educated guess based on the observational record from the nearby Weiherbach catchment on the same day.

To look at the feasibility of the transfer of rainfall intensities (Figure 3), we conducted additional simulations (Figure 5) with alternative rainfall distributions, including one derived from a radar observed 2016 event in the Elsenz Schwarzbach

TABLE 5 | Summary of the main NbS measures considered in our work.

Implementation	Parameter	Changes
Hedgerows in the middle of the area designated as crops in the representative hillslope	Gauckler-Manning-Strickler Coefficient (K_{st})	Reduced by 50% compared to landuse- crops
	Saturated hydraulic conductivity of the first 40 cm of soil (k_{sat})	Increased by an order of 2 compared to landuse- crops
	Saturated water content of the first 40 cm of soil (Θ_{sat})	Increased by 20% compared to landuse- crops
Practices aimed at minimising soil compaction for forest regions spanning the representative hillslope	Saturated hydraulic conductivity of the first 40 cm of soil (k_{sat})	Increased by an order of 1 compared to landuse-trees
	Saturated water content of the first 40 cm of soil (Θ_{sat})	Increased by 10% compared to landuse- trees

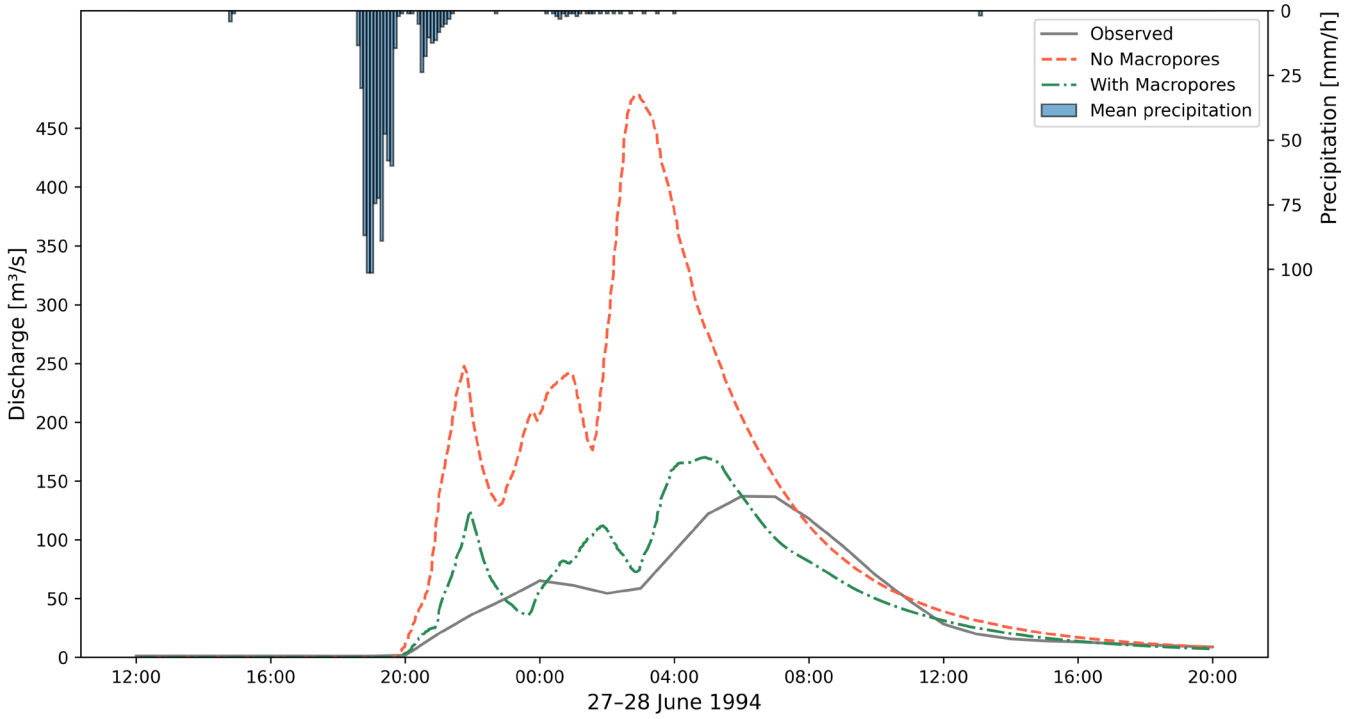

FIGURE 4 | Modelled hydrographs (smoothed 1-hourly windows) compared to the observed outlet time series. The green curve represents simulations with macropores, while the orange curve shows model run without considering any macropore flow.

TABLE 6 | Flood event characteristics at the outlet gauging station near Eschelbronn (Gauge A).

	27.06.1994		28.04.2023	
Flood metrics	**Flood volume (1000 m³)**	**Flood peak (m³/s)**	**Flood volume (1000 m³)**	**Flood peak (m³/s)**
Observed	4683.74	136.97	1146.35	24.31
Simulated	5276.64	170.06	1232.75	38.75
Relative Error (%)	−12.6	−24.2	−0.1	−59.4

catchment and another based on a synthetic triangular distribution of assumed duration of 2 h.

The simulation using the 2016 rainfall intensities produced a broadly comparable storm hydrograph, albeit with timing errors, likely because the 2016 event peaked earlier than the 1994 storm. In contrast, the simulation based on the synthetic distribution resulted in larger errors in both flood volume and peak discharge. Overall, the additional tests suggest that the transfer of intensities from nearby experimental catchments may provide a useful first approximation for investigating intensity-driven events in data-scarce regions, especially for historical storms where radar-based estimates are unfortunately not available. They also reveal that

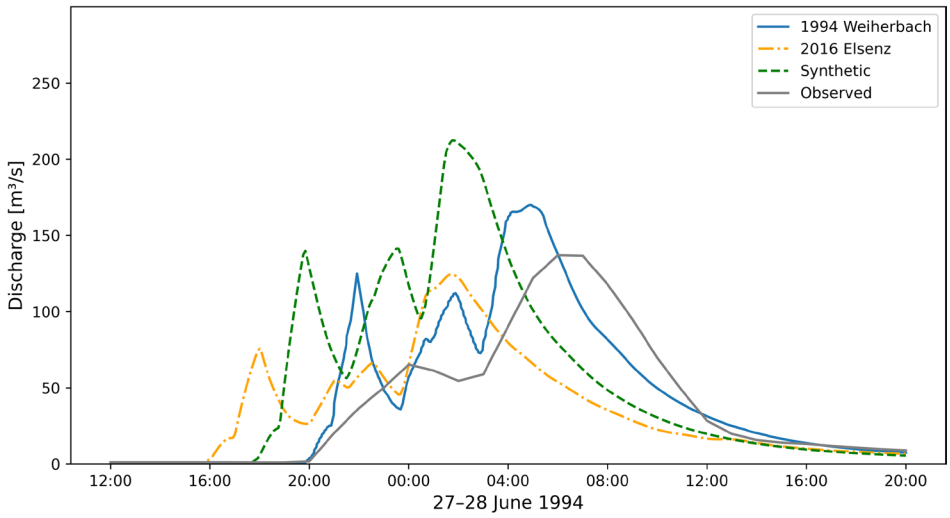

FIGURE 5 | Sensitivity of simulated flood response to the forcing intensities.

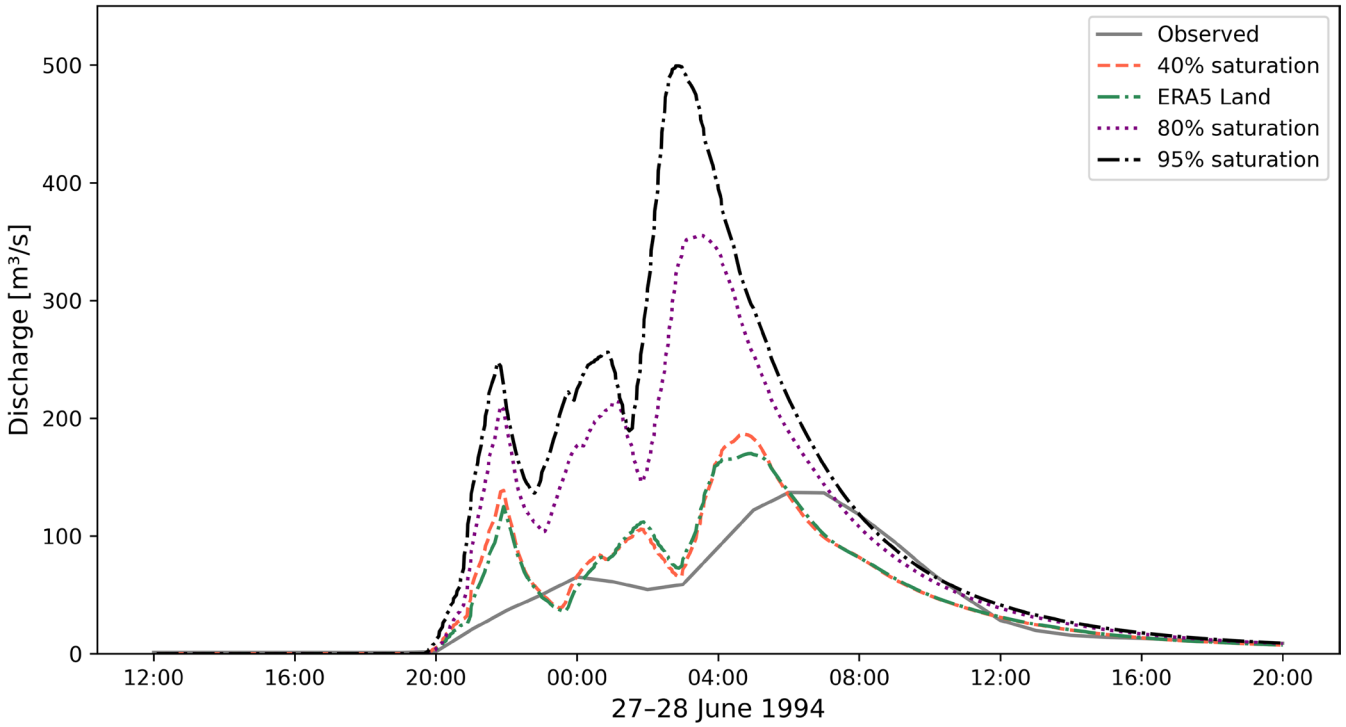

FIGURE 6 | Sensitivity of simulated flood response to varying antecedent soil moisture conditions.

such historical storms are not isolated occurrences; the storm in 2016 had a broadly similar pattern (with earlier peaks) to the one in 1994 and led to a similar catchment response.

Sensitivity analyses (Figure 6) for alternative antecedent soil moisture initialisations instead of ERA5 Land, demonstrate a strong control of antecedent wetness on flood response. This effect is probably intensified by the activation of preferential flow pathways, which depend on soil moisture conditions (Equation 2.5) within the hillslopes.

To again validate the performance of our model on another event, we simulated a flood (with far less intensities compared to the 1994 flood) event that occurred in April 2023. It is important to note that reservoirs introduce greater uncertainty into simulations of flood peaks in more recent periods, as they are now heavily regulated (Zweckverband Hochwasserschutz Elsenz-Schwarzbach 2016) and the present set-up does not account for reservoir operations at this stage. Our model run again showed low errors in the total flood volume (Table 6). However, the higher modelled flood peak led to greater relative errors in peak discharge.

4.2 | Reconstruction of the 1994 Flood

The model set up is then utilised to investigate the flooding within the Elsenz Schwazbach catchment during June 1994. While this historical flood led to widespread damage

(Figure B2) within the catchment, as recorded in grey literature (Henkel 1994; Vogt 2024), not much information is known about the relative storm volumes and peak values that hit the different population centres within the catchment.

The gauge near Neckarbischofsheim (Gauge B in Figure 1) records only flood-level markings, and because the observed level was higher than the established rating curve, it is not possible to derive the flood volume for this event from observations alone.

We compared the water level observations at Gauge B to the channel water levels modelled in our setup (Figure A3) at the nearest node. Figure 7A shows the simulated wave heights alongside the observed water levels. Although the model does not replicate the observed curve exactly, it satisfactorily captures the overall timing, magnitude, and recession behaviour. It is also important to consider the uncertainties in the observations, especially for such short-duration, high-impact events. While the observational records indicate that the peak occurred approximately 8 h after the flood began, experiences with rapid responses (up to 2–3 h) during such events in areas of this scale (catchment area up to Gauge B = 35 km^2) question the accuracy of the measurements during the flood.

Due to the flood gauge level markings being well outside the calibrated range of the rating curve, the official discharge record at Neckarbischofsheim is incomplete for this event. We used the model to predict the flood hydrograph till this point and compared it to the incomplete discharge record at the gauging station (Figure 7B). The high discharge values (around 100 m^3/s) and the successive flood waves explain the widespread destruction experienced at the city of Neckarbischofsheim during the evening on 27 June 1994. While newspaper records (Henkel 1994) and archival footage (Vogt 2024) highlights the impacts (Figure B2) felt; it was previously not possible to quantify the event's magnitude in hydrological terms.

The double peak nature of the flood hydrograph (Figure 7B) warrants a closer look at the smaller headwater catchments that drain to this city. We focused on two headwater subbasins (Figure A5 in Appendix A) that subsequently drain into the city of Neckarbischofsheim.

Subbasin 84 encompasses part of the city, which is situated at the foot of the basin. The impervious area in such downstream parts leads to low infiltration and, conversely, faster flow. This compounds the flood hazard for the city. As seen from the flood hydrograph (Figure 7C) for the subbasin, there is an abrupt rise in the rising limb, possibly due to the urban built up area downstream of the subbasin. The location of the agricultural plots upstream (Figure A5) in subbasin 84 also leads to more sediment and debris flow to the city, as seen from archived footage (Figure B2) of the aftermath of the flood in Neckarbischofsheim.

Subbasin 123 is located (Figure A5) just upstream of the town of Obergimpern; the basin is predominantly agricultural in nature with large open fields. The large open fields without any hedgerows or rills again exacerbate the flooding by allowing more sediment flow into the stream. The slower rising limb (Figure 7D), when compared to hillslope 84 (Figure 7C), suggests gradual overland flow generation with erosion, and also more mixing time for the suspended sediments in the channel. Analysing the individual responses reveals that the earlier and higher observed flood peak at Gauge B (Figure 7B) predominantly originates from the headstream regions (Subbasin 84), which drain directly into it. In contrast, the smaller second peak is associated with other catchments that flow into the city along the river network. The shorter travel duration between the two peaks indicates a scenario of temporal preconditioning and hazard cascading (Zscheischler et al. 2020), where the initial flood has already created a hazardous situation that is then worsened by the subsequent flood, leaving very little time for recovery or rehabilitation.

It is curious to note that the flood reservoir downstream (designed for a 100 year flood) of subbasin 123 was again overtopped (Figure B4) in the summer flood series of 2016 (Reservoir W22 in Manoj et al. 2024), raising interesting questions about the adequacy of existing design measures in response to increasing flash floods in a warming climate.

4.3 | Scenario Based Analysis of Flood Estimates

Using our model setup, we conducted scenario-based simulations for the entire Elsenz Schwarzbach catchment to explore flood responses associated with different return periods derived from standard design precipitation estimates (Table 4) provided by the German Weather Services (Junghänel et al. 2017). The initial conditions and storm duration were assumed to be the same as those of the 1994 summer flood. The simulated flood responses were then compared to the official statistical T-year return period floods currently established for planning and design practices for flood protection in the German state of Baden-Württemberg.

The comparison between simulated and design floods (Table 7) reveals generally close agreement at Gauge A (catchment outlet) across most return periods, with deviations within ±15% except for the 10 000-year event, where the flood is notably underestimated. In contrast, Gauge B shows substantial underestimation across all return periods, with errors exceeding 70%.

These results highlight a clear contrast: while design flood estimates at the larger outlet gauge are broadly consistent with the simulated T-year floods derived from extreme precipitation statistics, this correspondence is less evident at smaller gauging stations. This discrepancy may partly explain the overtopping of headwater reservoirs upstream of Neckarbischofsheim (Manoj et al. 2024) during the 2016 summer floods.

Overall, the findings suggest that current flood estimation approaches may be sensitive to intensity-driven events, particularly at smaller spatial scales. They also indicate that, while structural measures are often centralised and may be vulnerable under extreme conditions, distributed, non-structural nature-based measures could play a complementary role in mitigating flood impacts.

4.4 | Exploratory Analysis of Nature-Based Solutions

To explore the potential influence of NbS on flash flood response, we conducted a scenario-based numerical experiment

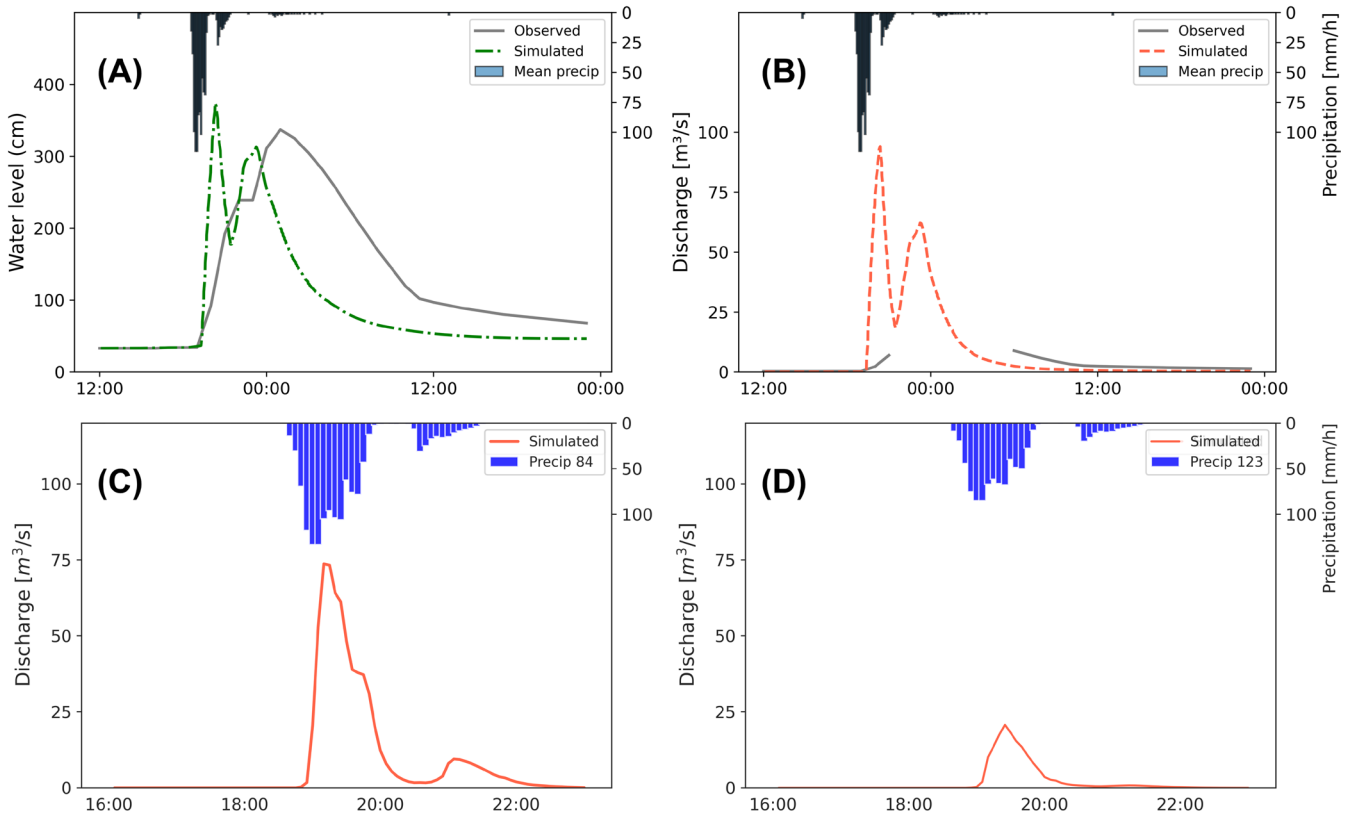

FIGURE 7 | Comparison between simulated (orange) and observed (grey) water levels at the Neckarbischofsheim gauge (A); reconstructed flood hydrograph at Neckarbischofsheim (B); simulated flood hydrograph for hillslope 84 during the June 1994 event (C); and simulated flood hydrograph for hillslope 123 during the June 1994 event (D).

TABLE 7 | Comparison of the simulated and standard design floods over the two gauging stations.

	Eschelbronn (Gauge A)			Neckarbischofsheim (Gauge B)		
Return period (years)	**Simulated**	**Design flood**	**Error (%)**	**Simulated**	**Design flood**	**Error (%)**
100	83.92	88.56	5.2	24.35	14.4	−69.1
200	96.73	99.2	2.5	27.98	16.4	−70.6
500	129.08	114	−13.2	35.22	19.2	−83.4
1000	141.8	125	−13.4	39.32	21.5	−82.9
10000	239.81	166	−44.5	63.04	29.9	−110.8

using our model setup (see Table 5), incorporating hedgerows and forest management practices in subbasins 84 and 123. The baseline scenario (Figure B3), which does not include NbS, was compared to a scenario in which these measures were implemented across the corresponding landuse classes within the representative hillslope profiles.

The NbS scenario (Figure 8) indicates reductions in both flood volume and peak discharge in the two subbasins. In subbasin 84, the relative volume reduction was approximately 6.5%, while peak discharge decreased by about 19%. These results suggest that the implemented NbS primarily influence the timing and magnitude of runoff rather than fundamentally altering the dominant runoff generation mechanisms. In this sense, they appear to act as local attenuation features, reducing peak discharge before water is routed to the channel network. For subbasin 123, the relative volume reduction was 19.6%, with a peak discharge reduction of 29.3%. At the further downstream outlet (Neckarbischofsheim gauge), these changes correspond to a simulated reduction of approximately 16 m^3/s (≈11%) in peak discharge and about 23 cm (≈6%) in peak water levels.

5 | Discussion

5.1 | Upscaling Vectorised Representation

Nearly 40 years after Dooge's seminal paper (Dooge 1986), which identified intermediate-scale catchments (up to 250 km^2) as systems of organised complexity, challenges remain in modelling flash flood responses (Collier 2007) driven by Hortonian overland flow at these scales. These catchments are too organised to

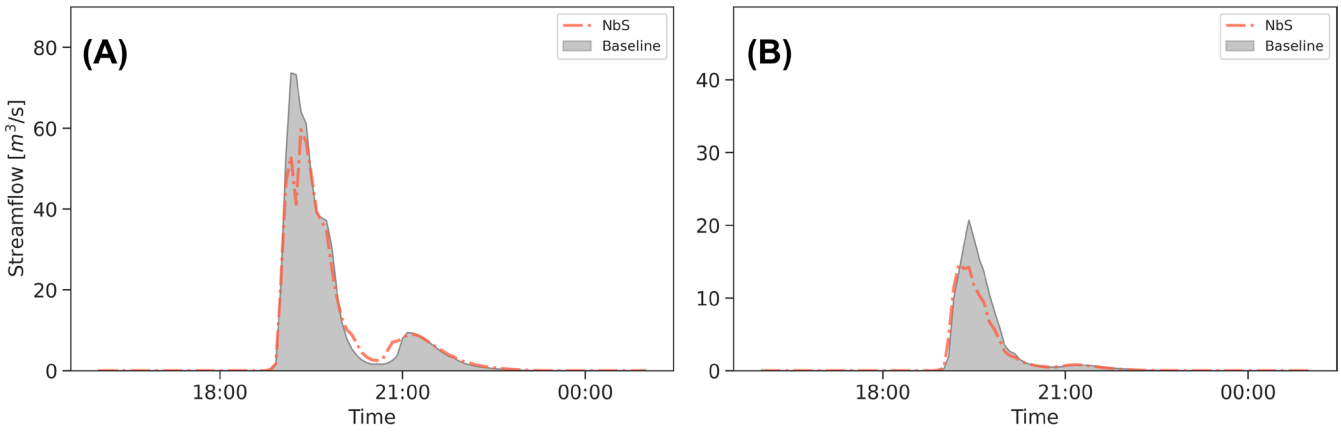

FIGURE 8 | Simulated effects of nature-based solutions (NbS) in subbasins 84 (A) and 123 (B).

be represented solely through statistical methods, yet too large and heterogeneous to be described in a deterministic manner. A key requirement (Zehe et al. 2014) at such scales is a better understanding and representation of how different forms of spatial organisation affect storage and release of water and energy. This is particularly important for threshold or emergent behaviour (Zehe and Sivapalan 2009) like onset of preferential flow (Beven and Germann 1982).

In this study, we test a coupled hydrological—hydraulic model at such an intermediate scale (196 km^2) relying on a vectorised representation of sub-catchments as representative hillslopes that maintains the total flow potential of a subbasin and then coupled it to a 1D kinematic wave module for flood routing along the main catchment. While the theory of representative hillslopes has attracted increased attention (Fan et al. 2019) here we show that the approach can be coupled with standard flow routing methods for reliable rainfall-runoff simulations at the meso-catchment scale.

We revisited the devastating Kraichgau flood events in Germany during the summer of 1994 using our modelling framework. Consistent with observations from other studies (Bronstert et al. 2023) investigating the role of preferential flow processes, we found an overestimation of event response when macropore flow was not represented. During intense convective storms, a substantial portion of incoming precipitation bypasses the soil matrix through such preferential flow paths. By incorporating macroporosity parameters from previous studies (Manoj et al. 2024; Niehoff et al. 2002) to account for these processes, we achieved a substantially improved representation of the event dynamics. This suggests that parameter transfer is a feasible approach for representing coupled flow processes in hydrological models across regions with similar hydrological characteristics.

It is important to stress that our model setup does not perfectly replicate the observed flood hydrographs. While the reconstructed event still shows an overestimation of approximately 24%, this can be partly attributed to the lack of local observational data, which required the transfer of storm intensities from the nearby Weiherbach catchment, as well as uncertainties introduced by the 1D routing approach, particularly for peak discharge. For the more recent event, the larger peak overestimation (≈59%) is likely influenced by the reduced actual flood discharge due to reservoir operations implemented after the 1994 event, which are not included in the current model setup. Importantly, the relatively small errors in total flood volume (≈1%–12%) demonstrate that the model captures the overall flood volume dynamics with reasonable consistency.

Our choice of the 1D kinematic wave routing to connect the vectorised representation for subbasins, based on energy gradients, does not imply that the processes at the channel scale are in any way less important for a comprehensive assessment of flood dynamics during such storms. Rather, this choice is motivated by the fact that a large number of well-tested hydraulic models (Fenton 2019) are available for channel routing. Often, the main limitation for achieving reliable predictions lies in the runoff generation aspect (Brunner et al. 2021), which determines how high-intensity rainfall during these events is translated into runoff. Our goal is to improve upon top-down approaches, such as the unit hydrograph and curve number methods, which have been found to be lacking in this context (Kirkby and Cerdà 2021).

5.2 | Enhancing Current Design Approaches

Significant advances have been made in climate physics and meteorology, particularly in modelling intense storms that align with the increased emission scenarios of anthropogenic climate change (IPCC 2021). However, these advancements have not led to improved estimates of design flood hydrographs. This limitation is partly due to the lack of well-suited hydrological models and gaps in data records, especially at smaller headwater catchment scales, which are ironically the areas most affected by flash floods.

Also, the number of gauges in small headwater catchments has decreased in recent decades, and most gauges are now disproportionately located in larger perennial rivers (Krabbenhoft et al. 2022). This drastically impacts our ability to understand what has happened and can happen at such crucial scales (Michelon et al. 2021). The current official 100-year flood estimate at the Neckarbischofsheim gauge is 14.4 m^3/s. The 1994 summer flood, having exceeded the rating curve range, was not incorporated into the dataset used for long-term statistical analysis, which led to an underestimation of flood quantiles at

the gauge. In this regard, event reconstruction can serve as a valuable tool to supplement observational records of extreme events and improve flood estimates across all return periods. Using our trained model, we reconstructed the flood values at Neckarbischofsheim. The high successive discharge peaks are in line with the large scale destruction reported in the town (Figure B2 in Appendix B) during 27–28 June 1994.

The normalised peak runoff values, expressed as the ratio of flood peak discharge to total catchment area, show good consistency across scales. For the catchment area up to Neckarbischofsheim, the reconstructed peak discharge of approximately 94 m^3/s over an area of 35 km^2 yields a specific discharge (2.68 $m^3/s/km^2$) comparable to that observed (Villinger et al. 2022) in the smaller, well-instrumented Weiherbach catchment (2.25 $m^3/s/km^2$) for the same storm during summer of 1994, where a peak discharge of 7.9 m^3/s was recorded over 3.5 km^2.

We also looked at the headwater catchments contributing to the runoff at the town to understand the hazard cascade for the event. Our main finding was that the spatial arrangement of settlements, located downstream of agricultural fields, makes them more vulnerable to the impacts of overland flow and debris flow from upstream areas. Considering such land-use patterns and their spatial organisation while planning new settlements in the region could help reduce the risk of similar events in the future.

We then compared simulations of floods with different T-year return periods to the currently recommended design standards and found that the underestimation errors were larger at smaller spatial scales. This is an important consideration to be made in the future design of small to medium flood reservoirs in the region. While the comparison was made to the regionalised statistical model (LUBW 2025) that relies on observed annual peak flood data and other catchment predictors currently commissioned in the federal state of Baden-Württemberg in Germany, similar models or statistical design floods exist for regions around the world.

While hydrologic non-stationarity (Milly et al. 2008) has been recognised for decades now, this hasn't yet translated into meaningful guidance for engineers and practitioners (Wasko et al. 2021). The intensification of sub-daily precipitation extremes (IPCC 2021) is a significant challenge, as current design approaches primarily focus on the total volume of the storm rather than the intensity dependence of runoff, especially for small- to medium-sized reservoirs. The design floods for the reservoirs in the Elsenz Schwarzbach catchment relied on a hydrological model (Ihringer 1994) employing the unit hydrograph and an empirical estimate of the runoff coefficient. This partly explains why quite a few of the reservoirs got overtopped during the intensity driven 2016 summer flash floods (caused by a 25-year rainfall), even though the reservoirs were designed for a 100-year flood.

5.3 | Revitalising Flood Protection

The headwater flood reservoirs in the Elsenz Schwarzbach, established after the disastrous flooding episodes in 1993–1994 were overtopped (Figure B4) during the convective storm clustering of summer 2016. This again calls for a relook into traditional structural flood protection measures and their benefits compared to decentralised flood protection. Although the combined area of subbasins 84 and 123 is only 6.73 km^2, which accounts for approximately 19% of the total catchment area of 34.75 km^2 leading up to the gauging station at Neckarbischofsheim, the flood peaks during the 1994 flood, especially the larger initial flood wave, were significantly influenced by the rapid runoff response in these two subbasins.

We conducted exploratory, scenario-based experiments in two headwater subbasins, implementing NbS within agricultural and forest land use classes by modifying key hydrological parameters in the hillslope model. The simulations indicate reductions in flood peaks at both the subbasin scale and at the downstream gauging station.

Our decision to use representative hillslopes for the subbasins in our study area enables us to effectively map land use classes based on their positions relative to the topographic gradient driving overland flow. Archival images (Figures B2 and B3) suggest considerable debris flow during the event, likely linked to the downstream location of population centres relative to agricultural fields and forests. The runoff responses observed in subbasins 84 and 123 highlight the importance of considering both the relative positions of land use types and their arrangement within modelling units.

For better meso-scale flood management, it is crucial to avoid the superimposition of peaks arising from runoff generation at the different parts of the catchment. A rather homogeneous landuse distribution implies a strong connectivity in the overland flow. Measures such as hedgerows in agricultural fields reduce connectivity, providing localised impediments, slowing Hortonian runoff, and increasing local infiltrability. The related valuable delays in the time to peak help runoff from adjacent fields not to reach the flood channel simultaneously. This could lead to downstream benefits along the river network.

5.4 | Limitations and Outlook

Modelling of hydrological systems has benefitted immensely from different complementary (and yet sometimes competing) modelling philosophies (Fatichi et al. 2016; Hrachowitz and Clark 2017). Our approach to scaling predictions to intermediate-scale catchments, using approximations that aim to conserve energy gradients, reproduces Hortonian runoff generation during a historical flood while addressing data scarcity. This method proves to be a valuable virtual laboratory for investigating design flood adequacies and different mitigation scenarios at such scales. However, certain limitations of the study warrant closer examination.

Our choice of hydrological model (CATFLOW—Zehe et al. 2001) is motivated by prior experience applying the model in similar landscapes. In theory, the concept of representative hillslopes is appropriate for use with any spatially distributed, physically based model (PARFLOW—Maxwell (2013), SERGHEI—Caviedes-Voullième et al. (2023) or HydroGeoSphere—Jones

et al. (2006)) that can explicitly account for the gradients represented by the hillslope geometry.

Regarding the study area, the Elsenz Schwarzbach was chosen as it provides an ideal testing ground for reconstructing a historical flood that had substantial socio-economic impacts, and because its population settlements are embedded within a mosaic of agricultural and forested land, which is well suited to evaluating the potential of NbS to mitigate flood-related damages. The locations of the catchment within the same hydro-pedological regime of an experimental catchment imply that we can opt for a transfer of soil hydraulic parameters and rely on literature values instead of calibration. It is important to note that these parameters could also be derived using soil pedotransfer functions based on openly available textural data. However, in this case, more events may be required for calibration. The macroporosity parameters, namely the scaling factor for saturated hydraulic conductivity and the extent of preferential flow dynamics in the representative hillslope element, were informed by our prior experience (Manoj et al. 2024) in simulating flood responses in agricultural loess soil catchments in the Kraichgau region. As demonstrated, these parameters are highly sensitive; therefore, direct transfer to other regions may not always be feasible, but can be guided by literature values and insights from studies in hydrologically similar settings. Due to the lack of high-resolution rainfall intensity data, we also transferred the rainfall hyetograph from the experimental Weiherbach catchment and applied this intensity distribution uniformly across all subbasins. This represents a strong assumption, as Hortonian overland flow is primarily controlled by rainfall intensity. Nevertheless, the model reproduces the main storm dynamics reasonably well compared to simulations using recent storms and synthetic distributions, suggesting that such a transfer may provide a useful first approximation for investigating intensity-driven events in data-scarce regions, especially for historical storms where radar-based estimates are unfortunately not available.

Concerning the experimental design, although the 1D kinematic wave for the hydraulic routing provides a simple yet computationally efficient framework that is adequate for reproducing the overall flow characteristics of the flood wave at the meso-catchment scale, this choice implies some important processes may not be sufficiently represented in our setup. During such intense events, overbank flow may occur, and water spreads onto the wide floodplains parallel to the channel. When the water leaves the main channel, there would be temporary storage on the floodplain and delayed return flow. These dynamics cannot be accurately captured by one-dimensional kinematic wave routing. This limitation may explain the more abrupt rise of the flood wave and the earlier recession seen in Figures 3 and 5a compared to observations. Leveraging advanced 2D flow routing solvers and linking them to the output hydrographs from the hillslope models could alleviate such shortcomings. This will also enhance the estimation of inundation maps for flood management planning scenarios, thereby bridging the gap between research and practice. The exploratory NbS analysis draws on parameter values from previous field studies on loess soils. However, additional factors such as hedgerow type, stem density, and growth stage may also affect the results. While the initial findings indicate a possible reduction in flood response, they should be regarded as a first step toward more detailed field and modelling studies on the effectiveness of NbS in the region's agricultural and forested landscapes.

6 | Conclusions

In this study, a mesoscale catchment model was applied to simulate rainfall–runoff response during a historical flash flood in southwest Germany. To preserve the local driving gradients of flow, we employed a simplification based on representative hillslopes derived from topographic information within each subbasin, which were subsequently coupled through hydraulic routing to simulate flood wave propagation across the catchment.

Results from the Elsenz Schwarzbach catchment suggest that this approach provides a feasible framework for analysing flash flood dynamics under the conditions considered. The gradient-based representation enables the inclusion of hydrologically relevant processes, such as preferential flow, while maintaining computational efficiency at the mesoscale, thereby offering a practical compromise between fully distributed and simplified conceptual modelling approaches.

The reconstructed event indicates that existing flood estimates at smaller spatial scales may be sensitive to the exclusion of extreme events, although this finding should be interpreted in light of the underlying assumptions. The exploratory nature-based solution (NbS) scenarios further suggest that localised, non-structural measures, such as hedgerows, may influence runoff generation and contribute to peak reduction under the simulated conditions. Overall, this study advances flash flood modelling at the mesoscale and provides a basis for further investigation under data-scarce conditions.

Acknowledgements

This research contributes to the ViTamins project (Invigorating Hydrological Science and Teaching: merging key Legacies with new Concepts and Paradigms), funded by the Volkswagen Foundation. The authors would like to thank Dominik Elfgang and the Landesanstalt für Umwelt Baden-Württemberg for sharing observational data from Eschelbronn and Neckarbischofsheim. The authors would also like to acknowledge Hans-Joachim Vogt, Neckarbischofsheim for sharing the archival flood footage shown in Appendix B. Ashish Manoj J would like to thank Mirko Mälicke and Alexander Dolich for helpful discussions regarding the pre-processing workflow. We also gratefully acknowledge the Open Access Publishing Fund of the Karlsruhe Institute of Technology (KIT). In preparing this work, the authors utilized Grammarly and ChatGPT solely to enhance their writing. After employing these tools, the authors carefully reviewed and edited the content as needed and accept full responsibility for the published article's content. Open Access funding enabled and organized by Projekt DEAL.

Funding

This work was supported by Volkswagen Foundation through the ViTamins project (Grant No. 9B 192/-1).

Conflicts of Interest

The authors declare no conflicts of interest.

Data Availability Statement

The model setup, code, and all simulation results from the experiments reported in this study are archived at Manoj (2025). The GIS preprocessing workflow used in this study is based on https://github.com/VForWaTer/tool_whiteboxgis and archived at Manoj et al. (2025). The terrain and other input preprocessing for the CATFLOW model are based on https://github.com/VForWaTer/tool_catflow and archived at Manoj and Dolich (2025).

References

Auerswald, K., J. Geist, J. N. Quinton, and P. Fiener. 2025. "HESS Opinions: Floods and Droughts – Are Land Use, Soil Management, and Landscape Hydrology More Significant Drivers Than Increasing CO_2?" *Hydrology and Earth System Sciences* 29: 2185–2200. https://doi.org/10.5194/hess-29-2185-2025.

Beck, H. E., N. E. Zimmermann, T. R. McVicar, N. Vergopolan, A. Berg, and E. F. Wood. 2018. "Present and Future köppen-Geiger Climate Classification Maps at 1-Km Resolution." *Scientific Data* 5: 180214. https://doi.org/10.1038/sdata.2018.214.

Beven, K., and P. Germann. 1982. "Macropores and Water-Flow in Soils." *Water Resources Research* 18, no. 5: 1311–1325. https://doi.org/10.1029/WR018i005p01311.

Boettiger, C. 2015. "An Introduction to Docker for Reproducible Research." *ACM SIGOPS Operating Systems Review* 49: 71–79. https://doi.org/10.1145/2723872.2723882.

Bronstert, A., D. Niehoff, and G. R. Schiffler. 2023. "Modelling Infiltration and Infiltration Excess: The Importance of Fast and Local Processes." *Hydrological Processes* 37: 1–20. https://doi.org/10.1002/hyp.14875.

Brown, C. F., S. P. Brumby, B. Guzder-Williams, et al. 2022. "Dynamic World, Near Real-Time Global 10 m Land Use Land Cover Mapping." *Scientific Data* 9: 1–17. https://doi.org/10.1038/s41597-022-01307-4.

Brunner, M. I., L. Slater, L. M. Tallaksen, and M. Clark. 2021. "Challenges in Modeling and Predicting Floods and Droughts: A Review." *Wiley Interdisciplinary Reviews Water* 8: 1–32. https://doi.org/10.1002/wat2.1520.

Brus, D. J., and J. J. H. van den Akker. 2018. "How Serious a Problem Is Subsoil Compaction in The Netherlands? A Survey Based on Probability Sampling." *Soil* 4: 37–45. https://doi.org/10.5194/soil-4-37-2018.

Caviedes-Voullième, D., M. Morales-Hernández, M. R. Norman, and I. Özgen-Xian. 2023. "SERGHEI (SERGHEI-SWE) v1.0: A Performance-Portable High-Performance Parallel-Computing Shallow-Water Solver for Hydrology and Environmental Hydraulics." *Geoscientific Model Development* 16: 977–1008. https://doi.org/10.5194/gmd-16-977-2023.

Cochrane, T. A., and D. C. Flanagan. 2003. "Representative Hillslope Methods for Applying the WEPP Model With Dems and GIS." *Transactions of ASAE* 46: 1041. https://doi.org/10.13031/2013.13966.

Collier, C. G. 2007. "Flash Flood Forecasting: What Are the Limits of Predictability?" *Quarterly Journal of the Royal Meteorological Society* 133: 3–23. https://doi.org/10.1002/qj.29.

Disse, M., and H. Engel. 2001. "Flood Events in the Rhine Basin: Genesis, Influences and Mitigation." *Natural Hazards* 23: 271–290. https://doi.org/10.1023/A:1011142402374.

Dooge, J. C. I. 1986. "Looking for Hydrologic Laws." *Water Resources Research* 22, no. 9S: 46S–58S. https://doi.org/10.1029/WR022i09Sp0046S.

Dunne, T. 1978. *Field Studies of Hillslope Flow Processes-"Hillslope Hydrology"*, edited by M. J. Kirkby, 227–293. John Wiley & Sons.

DWD. 2021. "Radolan [WWW Document]." Accessed January 12, 2025. https://www.dwd.de/DE/leistungen/radolan/radolan.html.

DWD. 2023. "Kostra-Dwd [WWW Document]." Accessed January 12, 2025. https://www.dwd.de/DE/leistungen/kostra_dwd_rasterwerte/kostra_dwd_rasterwerte.html.

DWD. 2024. "HYRAS-DE-PRE: Raster Data Set of Daily Sums of Precipitation in Mm for Germany – HYRAS-DE-PRE." Accessed December 1, 2025. https://opendata.dwd.de/climate_environment/CDC/grids_germany/daily/hyras_de/precipitation/.

Fan, Y., M. Clark, D. M. Lawrence, et al. 2019. "Hillslope Hydrology in Global Change Research and Earth System Modeling." *Water Resources Research* 55: 1737–1772. https://doi.org/10.1029/2018WR023903.

Fatichi, S., E. R. Vivoni, F. L. Ogden, et al. 2016. "An Overview of Current Applications, Challenges, and Future Trends in Distributed Process-Based Models in Hydrology." *Journal of Hydrology* 537: 45–60. https://doi.org/10.1016/j.jhydrol.2016.03.026.

Fenton, J. D. 2019. "Flood Routing Methods." *Journal of Hydrology* 570: 251–264. https://doi.org/10.1016/j.jhydrol.2019.01.006.

Francke, T., A. Güntner, G. Mamede, E. N. Müller, and A. Bronstert. 2008. "Automated Catena-Based Discretization of Landscapes for the Derivation of Hydrological Modelling Units." *International Journal of Geographical Information Science* 22: 111–132. https://doi.org/10.1080/13658810701300873.

Guillaume, B., A. Michez, and A. Degré. 2025. "Leveraging Soil Diversity to Mitigate Hydrological Extremes With Nature-Based Solutions in Productive Catchments: An Application and Insights Into the Way Forward." *Hydrology and Earth System Sciences* 29, no. 18: 4661–4688. https://doi.org/10.5194/hess-29-4661-2025.

Hager, W. H. 2015. "Albert Strickler: His Life and Work." *Journal of Hydraulic Engineering* 141: 1–5. https://doi.org/10.1061/(ASCE)HY.1943-7900.0001000.

Heldmyer, A., B. Livneh, J. Mccreight, L. Read, J. Kasprzyk, and T. Minear. 2022. "Evaluation of a New Observationally Based Channel Parameterization for the National Water Model." *Hydrology and Earth System Sciences* 26: 6121–6136. https://doi.org/10.5194/hess-26-6121-2022.

Henkel, P. 1994. *Der Mensch und das Schalten und Walten der Natur*. Frankfurter Rundschau.

Ho, S. Q.-G., R. Lang, and U. Ehret. 2025. "Forecast-Based Operation of Re-Purposed Small Reservoirs for Floods, Farms, and (Low) Flows." *EGUsphere* 2025: 1–28. https://doi.org/10.5194/egusphere-2025-4739.

Horton, R. E. 1933. "The Role of Infiltration in the Hydrologic Cycle. Eos." *Transactions of the American Geophysical Union* 14: 446–460. https://doi.org/10.1029/TR014i001p00446.

Hrachowitz, M., and M. P. Clark. 2017. "HESS Opinions: The Complementary Merits of Competing Modelling Philosophies in Hydrology." *Hydrology and Earth System Sciences* 21: 3953–3973. https://doi.org/10.5194/hess-21-3953-2017.

Ihringer, J. 1994. "Aufbau und Anwendung des Flußgebietsmodells "FGM." DVWK Fortbildungslehrgang Hydrol." In *Niederschlag-Abfluß-Modelle Für Kleine Einzugsgebiete Und Ihre Anwendung*. DVWK Fortbildungslehrgang Hydrol. https://pd.lubw.de/10187.

IPCC. 2021. *Climate Change 2021: The Physical Science Basis. Contribution of Working Group I to the Sixth Assessment Report of the Intergovernmental Panel on Climate Change*. edited by V. Masson-Delmotte, P. Zhai, A. Pirani, et al., 3949. Cambridge University Press. https://www.ipcc.ch/report/ar6/wg1/downloads/report/IPCC_AR6_WGI_Full_Report.pdf.

Jones, J. P., E. A. Sudicky, A. E. Brookfield, and Y.-J. Park. 2006. "An Assessment of the Tracer-Based Approach to Quantifying Groundwater Contributions to Streamflow." *Water Resources Research* 42. https://doi.org/10.1029/2005WR004130.

Junghänel, T., H. Ertel, and T. Deutschländer. 2017. "KOSTRA-DWD-2010R. Bericht zur Revision der koordinierten Starkregenregionalisierung

und-auswertung des Deutschen Wetterdienstes in der Version 2010." In *KOSTRA-DWD-2010R-Bericht zur Revis*, 2010. der Koord. Starkregenregionalisierung und -auswertung des Dtsch.

Kirkby, M., and A. Cerdà. 2021. "Following the Curve? Reviewing the Physical Basis of the SCS Curve Number Method for Estimating Storm Runoff." *Hydrological Processes* 35. https://doi.org/10.1002/hyp.14404.

Krabbenhoft, C. A., G. H. Allen, P. Lin, et al. 2022. "Assessing Placement Bias of the Global River Gauge Network." *Nature Sustainability* 5: 586–592. https://doi.org/10.1038/s41893-022-00873-0.

Lindsay, J. B. 2014. "The Whitebox Geospatial Analysis Tools Project and Open-Access GIS." In Proceedings of the GIS Research UK 22nd Annual Conference, University of Glasgow.

Liu, L., Y. Ren, Z. Li, and L. Zhou. 2025. "Enhancing Hydrological Modelling With Reanalysis Soil Moisture: A Data-Driven Approach for Optimizing Initial Conditions Through Reanalysis Integration." *Advances in Water Resources* 203: 105023. https://doi.org/10.1016/j.advwatres.2025.105023.

Loritz, R., S. K. Hassler, C. Jackisch, et al. 2017. "Picturing and Modeling Catchments by Representative Hillslopes." *Hydrology and Earth System Sciences* 21: 1225–1249. https://doi.org/10.5194/hess-21-1225-2017.

LUBW. 2007. *Arbeitshilfe zur DIN 19700 für Hochwasserrückhaltebecken in Baden-Württemberg*. Landesanstalt für Umwelt Baden-Württemberg. https://pd.lubw.de/93810.

LUBW. 2023. "Extremereignis (T>100 a) Für Anlagensicherheit Und Hochwasserschutz [WWW Document]." Accessed November 12, 2025. https://registry.gdi-de.org/id/de.bw.lubw.mdk/EE363459-509A-4967-8A81-060A21D1E9D5.

LUBW. 2025. *Abfluss-BW: Regionalisierte Abfluss-Kennwerte Baden-Württemberg*. Landesanstalt für Umwelt Baden-Württemberg.

Mälicke, M. 2024. "From Method Development to Software Integration: A Comprehensive Approach to Geostatistical Variogram Uncertainty." *Karlsruher Institut für Technologie (KIT)*. https://doi.org/10.5445/IR/1000172259.

Manoj, J. A. 2025. "Simulation Results and Model for Manoj J et al (2026)." Zenodo. https://doi.org/10.5281/zenodo.17828416.

Manoj, J. A., and A. Dolich. 2025. "Vforwater/Tool_Catflow: Release With Option Soil Support (V0.9.5)." Zenodo. https://doi.org/10.5281/zenodo.17988248.

Manoj, J. A., R. Loritz, F. Villinger, et al. 2024. "Toward Flash Flood Modeling Using Gradient Resolving Representative Hillslopes." *Water Resources Research* 60. https://doi.org/10.1029/2023WR036420.

Manoj, J. A., M. Mälicke, and A. Dolich. 2025. "Vforwater/Tool_Whiteboxgis: Updated Input for Mosaic Tool." Zenodo. https://doi.org/10.5281/zenodo.16980463.

Maxwell, R. M. 2013. "A Terrain-Following Grid Transform and Preconditioner for Parallel, Large-Scale, Integrated Hydrologic Modeling." *Advances in Water Resources* 53: 109–117. https://doi.org/10.1016/j.advwatres.2012.10.001.

Merz, B., G. Blöschl, S. Vorogushyn, et al. 2021. "Causes, Impacts and Patterns of Disastrous River Floods." *Nature Reviews Earth and Environment* 2: 592–609. https://doi.org/10.1038/s43017-021-00195-3.

Meyer, J., M. Neuper, L. Mathias, E. Zehe, and L. Pfister. 2022. "Atmospheric Conditions Favouring Extreme Precipitation and Flash Floods in Temperate Regions of Europe." *Hydrology and Earth System Sciences* 26: 6163–6183. https://doi.org/10.5194/hess-26-6163-2022.

Michelon, A., L. Benoit, H. Beria, N. Ceperley, and B. Schaefli. 2021. "Benefits From High-Density Rain Gauge Observations for Hydrological Response Analysis in a Small Alpine Catchment." *Hydrology and Earth System Sciences* 25: 2301–2325. https://doi.org/10.5194/hess-25-2301-2021.

Milly, P. C. D., J. Betancourt, M. Falkenmark, et al. 2008. "Climate Change: Stationarity Is Dead: Whither Water Management?" *Science* 80, no. 319: 573–574. https://doi.org/10.1126/science.1151915.

Mishra, A., S. Mukherjee, B. Merz, et al. 2022. "An Overview of Flood Concepts, Challenges, and Future Directions." *Journal of Hydrologic Engineering* 27: 1–30. https://doi.org/10.1061/(asce)he.1943-5584.0002164.

Mualem, Y. 1976. "A New Model for Predicting the Hydraulic Conductivity of Unsaturated Porous Media." *Water Resources Research* 12: 513–522. https://doi.org/10.1029/WR012i003p00513.

Muñoz-Sabater, J., E. Dutra, A. Agustí-Panareda, et al. 2021. "ERA5-Land: A State-Of-The-Art Global Reanalysis Dataset for Land Applications." *Earth System Science Data* 13: 4349–4383. https://doi.org/10.5194/essd-13-4349-2021.

Nash, J. E. 1957. "The Form of the Instantaneous Unit Hydrograph." Paper presented at proceedings of the International Association of Hydrological Sciences (IAHS), Toronto Ontario.

Nash, J. E., and J. V. Sutcliffe. 1970. "River Flow Forecasting Through Conceptual Models. Part I-a Discussion of Principles." *Journal of Hydrology* 27: 282–290. https://doi.org/10.1016/0022-1694(70)90255-6.

Nature Editors. 2012. "Must Try Harder." *Nature* 483: 509. https://doi.org/10.1038/483509a.

Niehoff, D., U. Fritsch, and A. Bronstert. 2002. "Land-Use Impacts on Storm-Runoff Generation: Scenarios of Land-Use Change and Simulation of Hydrological Response in a Meso-Scale Catchment in SW-Germany." *Journal of Hydrology* 267: 80–93. https://doi.org/10.1016/S0022-1694(02)00142-7.

Pall, P., M. R. Allen, and D. A. Stone. 2007. "Testing the Clausius–Clapeyron Constraint on Changes in Extreme Precipitation Under CO_2 Warming." *Climate Dynamics* 28: 351–363. https://doi.org/10.1007/s00382-006-0180-2.

Peters, A., T. L. Hohenbrink, S. C. Iden, and W. Durner. 2021. "A Simple Model to Predict Hydraulic Conductivity in Medium to Dry Soil From the Water Retention Curve." *Water Resources Research* 57. https://doi.org/10.1029/2020WR029211.

Rauthe, M., H. Steiner, U. Riediger, A. Mazurkiewicz, and A. Gratzki. 2013. "A Central European Precipitation Climatology-Part I: Generation and Validation of a High-Resolution Gridded Daily Data Set (HYRAS)." *Meteorologische Zeitschrift* 22: 235–256. https://doi.org/10.1127/0941-2948/2013/0436.

Richet, J.-B., J.-F. Ouvry, and M. Saunier. 2017. "The Role of Vegetative Barriers Such as Fascines and Dense Shrub Hedges in Catchment Management to Reduce Runoff and Erosion Effects: Experimental Evidence of Efficiency, and Conditions of Use." *Ecological Engineering* 103: 455–469. https://doi.org/10.1016/j.ecoleng.2016.08.008.

Rosier, I., J. Diels, B. Somers, and J. Van Orshoven. 2023. "The Impact of Vegetated Landscape Elements on Runoff in a Small Agricultural Watershed: A Modelling Study." *Journal of Hydrology* 617: 129144. https://doi.org/10.1016/j.jhydrol.2023.129144.

Rosier, I., J. Diels, B. Somers, and J. Van Orshoven. 2024. "Maximising Runoff Retention by Vegetated Landscape Elements Positioned Through Spatial Optimisation." *Landscape and Urban Planning* 243: 104968. https://doi.org/10.1016/j.landurbplan.2023.104968.

Ruiter, M. C., A. Couasnon, M. J. C. Homberg, J. E. Daniell, J. C. Gill, and P. J. Ward. 2020. "Why we Can No Longer Ignore Consecutive Disasters." *Earth's Future* 8: 1425. https://doi.org/10.1029/2019EF001425.

Schneider, F., and A. Don. 2019. "Root-Restricting Layers in German Agricultural Soils. Part I: Extent and Cause." *Plant and Soil* 442: 433–451. https://doi.org/10.1007/s11104-019-04185-9.

Strahler, A. N. 1957. "Quantitative Analysis of Watershed Geomorphology." *Eos, Transactions of the American Geophysical Union* 38: 913–920. https://doi.org/10.1029/TR038i006p00913.

Tang, Y. K., and R. W. Skaggs. 1977. "Experimental Evaluation of Theoretical Solutions for Subsurface Drainage and Irrigation." *Water Resources Research* 13: 957–965. https://doi.org/10.1029/WR013i006p00957.

Te Chow, V. 1959. *Open Channel Hydraulics*. McGraw-Hill Professional.

Troy, T. J., N. Devineni, C. H. R. Lima, and U. Lall. 2025. "Can Runoff Modeled at Coarse Resolution Simulate Floods at Finer Resolutions? A Case Study Over the Ohio River Basin." *Advances in Water Resources* 206: 105151. https://doi.org/10.1016/j.advwatres.2025.105151.

United States Geological Survey. 1989. *Guide for Selecting Manning's Roughness Coefficients for Natural Channels and Flood Plains*.

van Genuchten, M. T. 1980. "A Closed-Form Equation for Predicting the Hydraulic Conductivity of Unsaturated Soils." *Soil Science Society of America Journal* 44: 892–898. https://doi.org/10.2136/sssaj1980.03615995004400050002x.

Villinger, F., R. Loritz, and E. Zehe. 2022. "Torrents in Small Rural Catchments and the Potential of Physics-Based Models for Their Simulation." *Hydrologie Und Wasserbewirtschaftung* 66: 284–285. https://doi.org/10.5675/HyWa_2022.6_1.

Vogt, H.-J. 2024. "Das Hochwasser in Neckarbischofsheim 1994 [WWW Document]." Youtube https://www.youtube.com/watch?v=cPxJu-9h17A.

Wasko, C., S. Westra, R. Nathan, et al. 2021. "Incorporating Climate Change in Flood Estimation Guidance." *Philosophical Transactions of the Royal Society A - Mathematical Physical and Engineering Sciences* 379: 20190548. https://doi.org/10.1098/rsta.2019.0548.

Weiler, M. 2006. "An Infiltration Model Based on Flow Variability in Macropores: Development, Sensitivity Analysis and Applications." *Journal of Hydrology* 310: 294–315. https://doi.org/10.1016/j.jhydrol.2005.01.010.

Wienhofer, J., and E. Zehe. 2014. "Predicting Subsurface Stormflow Response of a Forested Hillslope-The Role of Connected Flow Paths." *Hydrology and Earth System Sciences* 18: 121–138. https://doi.org/10.5194/hess-18-121-2014.

Zehe, E., U. Ehret, L. Pfister, et al. 2014. "HESS Opinions: From Response Units to Functional Units: A Thermodynamic Reinterpretation of the HRU Concept to Link Spatial Organization and Functioning of Intermediate Scale Catchments." *Hydrology and Earth System Sciences* 18: 4635–4655. https://doi.org/10.5194/hess-18-4635-2014.

Zehe, E., T. Maurer, J. Ihringer, and E. Plate. 2001. "Modeling Water Flow and Mass Transport in a Loess Catchment." *Physics and Chemistry of the Earth, Part B: Hydrology, Oceans and Atmosphere* 26: 487–507. https://doi.org/10.1016/S1464-1909(01)00041-7.

Zehe, E., and M. Sivapalan. 2009. "Threshold Behaviour in Hydrological Systems as (Human) Geo-Ecosystems: Manifestations, Controls, Implications." *Hydrology and Earth System Sciences* 13: 1273–1297. https://doi.org/10.5194/hess-13-1273-2009.

Zscheischler, J., O. Martius, S. Westra, et al. 2020. "A Typology of Compound Weather and Climate Events." *Nature Reviews Earth and Environment* 1: 333–347. https://doi.org/10.1038/s43017-020-0060-z.

Zweckverband Hochwasserschutz Elsenz-Schwarzbach. 2016. "Elsenz-Schwarzbach Water Board [WWW Document]." https://www.zvhws.de/.

Appendix A

Elsenz Schwarzbach Catchment

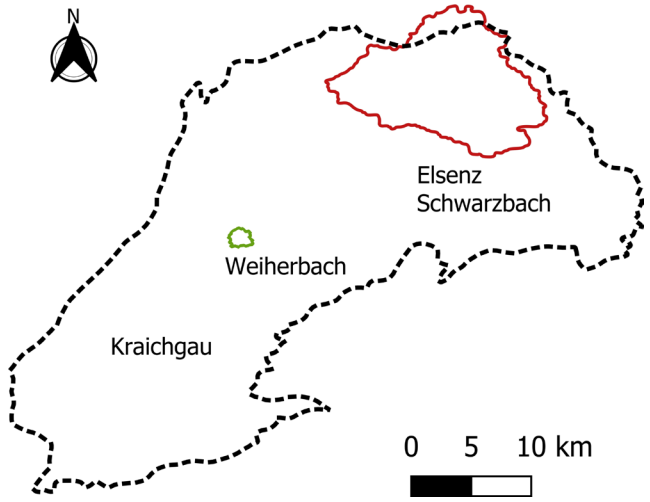

FIGURE A1 | Catchments Weiherbach and Elsenz Schwarzbach.

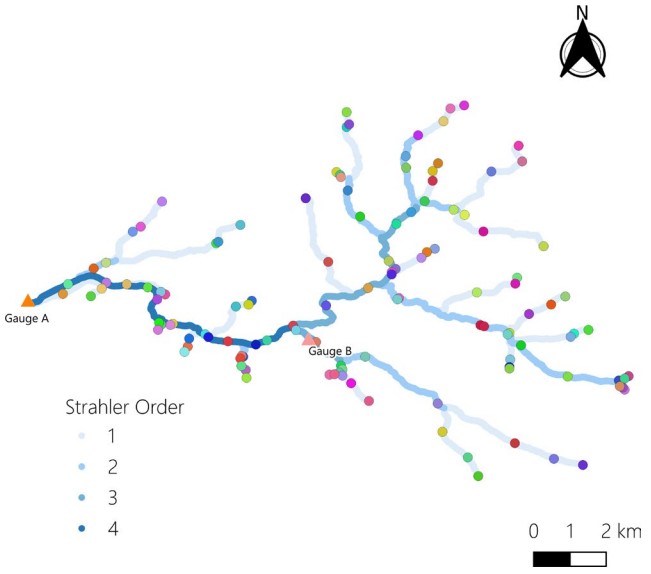

FIGURE A3 | Stream network used for routing within the catchment, along with the location of the outlets at which each representative hillslope is connected.

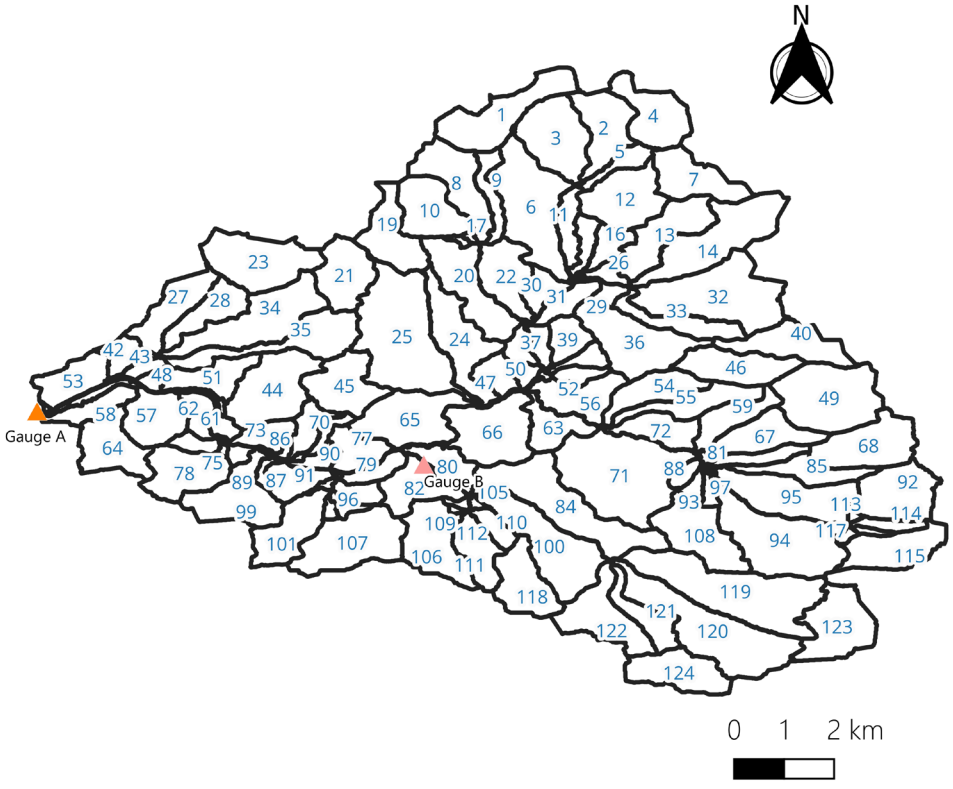

FIGURE A2 | Subbasins of the Elsenz Schwarzbach.

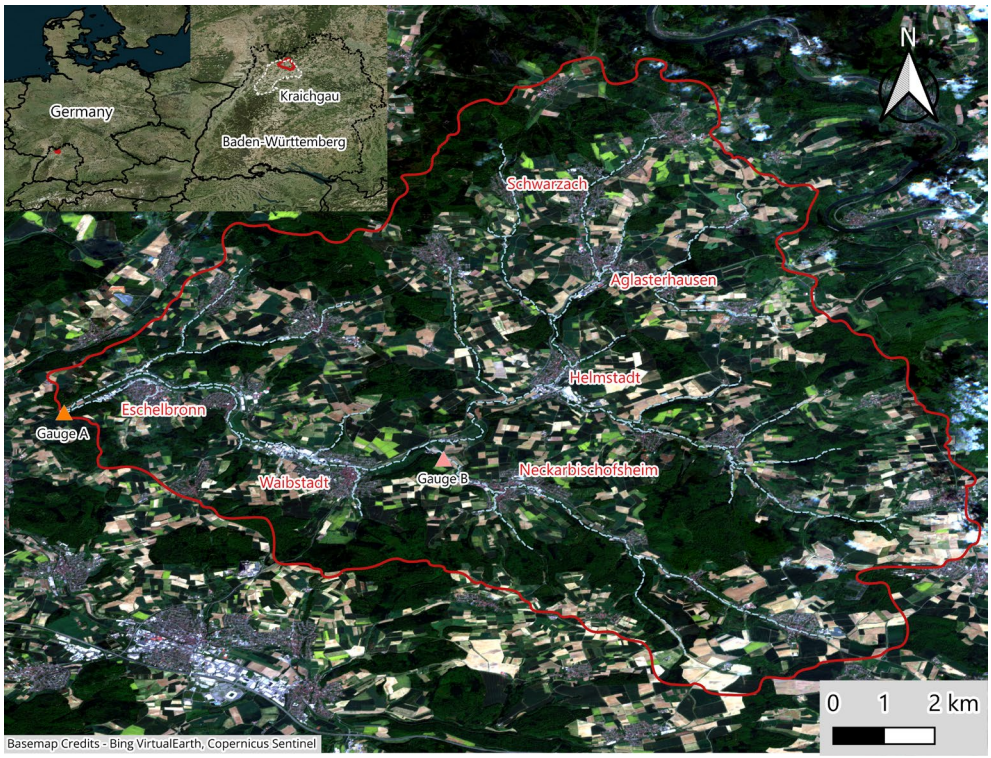

FIGURE A4 | Sentinel satellite image of the Elsenz–Schwarzbach catchment, highlighting spatial patterns of land cover.

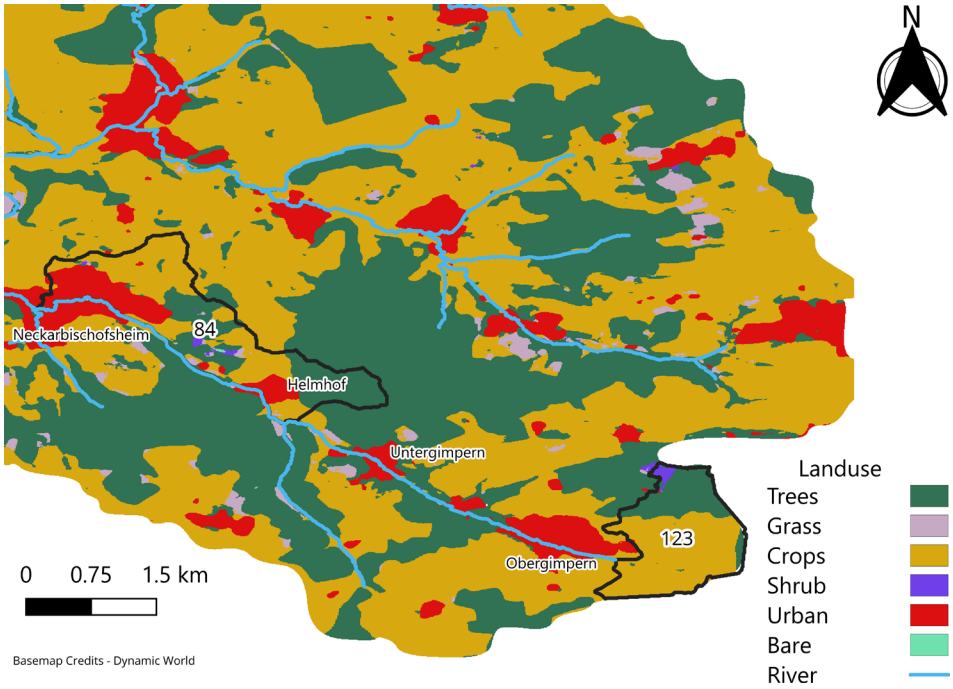

FIGURE A5 | Headwater subbasins 84 and 123, which drain to the city of Neckarbischofsheim.

FIGURE A6 | Locations within the Elsenz–Schwarzbach catchment: (A) Eschelbronn near the outlet gauging station, (B) Aglasterhausen in the headwater region, and (C) a flood regulating structure at Waibstadt. (Field visit on 02 August 2025).

Appendix B

Flood Events in the Elsenz Schwarzbach

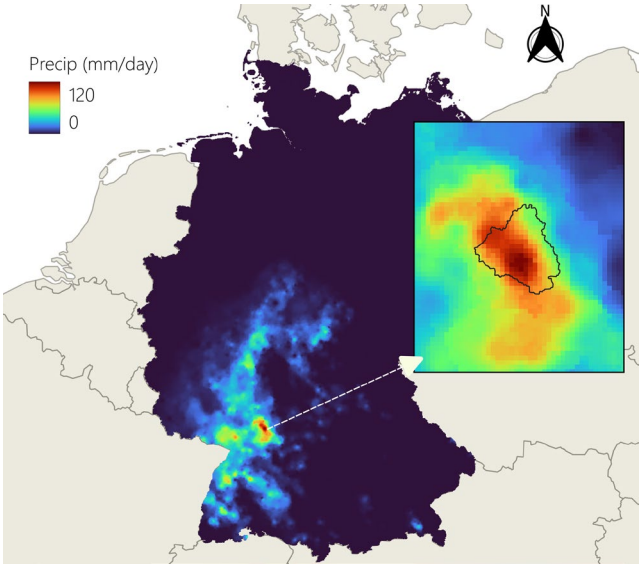

FIGURE B1 | Daily accumulated precipitation (06:00 UTC to 06:00 UTC the following day) from the HYRAS gridded product of the German Weather Service (DWD) for 27 June 1994 over Germany. The inset highlights the convective storm centre in the Elsenz–Schwarzbach catchment.

FIGURE B2 | Aftermath of 27 June 1994 flash floods over the Elsenz Schwarzbach (Image credit: Archiv Neckarbischofsheim).

FIGURE B3 | Flood evolution (27.06.1994) over agricultural landscapes in the Elsenz–Schwarzbach catchment. Archival flood footage (Vogt 2024) highlights extensive open fields and the absence of vegetative barriers in the affected area (Image credit: Archiv Neckarbischofsheim).

FIGURE B4 | Impact of flash floods on 08.06.2016 over Elsenz Schwarzbach (Image credit: Zweckverband Hochwasserschutz Elsenz-Schwarzbach).

Appendix C

Model Preprocessing

In this study, we utilise Docker containers (Boettiger 2015) to preprocess terrain data for the CATFLOW hydrological model (Figure C1). Docker is a containerization technology that packages software along with everything needed to run it—code, libraries, and system tools. This approach ensures consistent behaviour across different computers and users, representing a significant step toward computational reproducibility (Mälicke 2024; Nature Editors 2012).

We first employed containerized tool *tool_whiteboxgis* (Manoj et al. 2025) for the GIS preprocessing of the Digital Elevation Model (DEM) data. This tool wraps the open-source platform WhiteboxTools (Lindsay 2014) for geospatial analysis. The *tool_whiteboxgis* prepares standard raster files, such as aspect, elevation, and distance, which can then be used directly to derive the required terrain files for the hydrological model CATFLOW.

These raster files are then used as inputs for *tool_catflow* (Manoj and Dolich 2025). To derive the hillslope profiles for each sub-catchment in the study area, we run *tool_catflow* in parallel to ensure fast, efficient processing. Each sub-catchment is processed in its own container, thus providing modularity (Boettiger 2015) in both programming and hydrological sense. The relevant code and software are finally archived in Zenodo (Manoj et al. 2025; Manoj and Dolich 2025) for reusability.

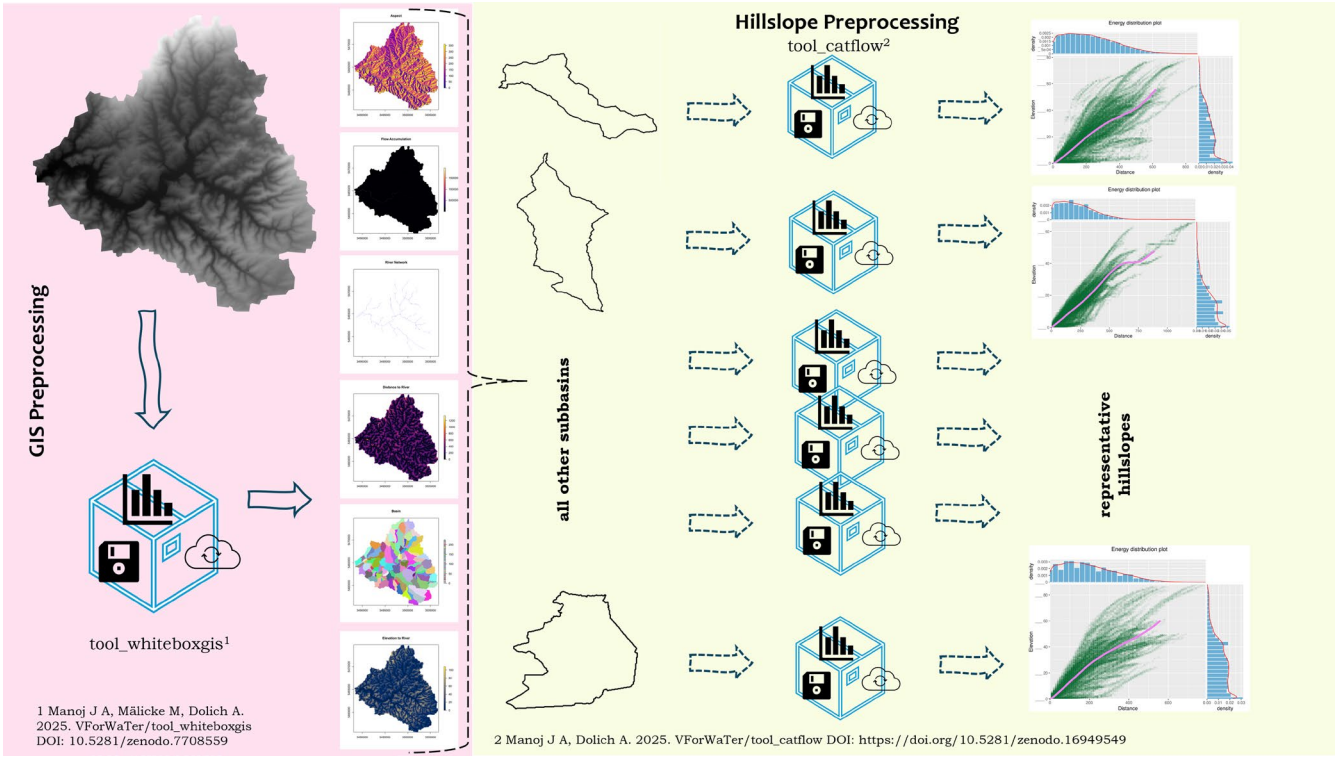

FIGURE C1 | Brief overview of the preprocessing workflow.